Escola d'Enginyeria de Telecomunicació i Aeroespacial de Castelldefels

UNIVERSITAT POLITÈCNICA DE CATALUNYA

POLITECNICO DI TORINO

TREBALL FINAL DE GRAU

TFG TITLE: Study of a simplified friction joint for the identification of the contact stiffness

DEGREE: Grau en Enginyeria de Sistemes Aeroespacials

AUTHOR: Irene Rodríguez Gauxachs

DIRECTORS: Christian Maria Firrone, Jose Ignacio Rojas Gregorio

DATE: July 17, 2020

Título: Study of a simplified friction joint for the identification of the contact stiffness

Autora: Irene Rodríguez Gauxachs

Directores: Christian Maria Firrone, Jose Ignacio Rojas Gregorio

Fecha: 17 de Julio del 2020

Resumen

Las palas de turbina usan normalmente articulaciones mecánicas para adjuntar la pala en el disco de la turbina. En este tipo de articulaciones, los problemas de contacto son muy comunes. Se les llama problemas de contacto porque ocurren donde dos superficies localizadas están en contacto y se distingue un comportamiento peculiar en comparación al comportamiento global de la estructura debido a presiones elevadas o efectos relacionados con la fricción. En algunos casos, el comportamiento específico de la zona de contacto puede afectar al comportamiento global de la estructura y no puede ser negligido: desde el punto de vista estático, pueden aparecer posibles intensificaciones de tensiones que pueden provocar fallos, y desde el punto de vista dinámico, la articulación puede actuar como una restricción y en consecuencia el contacto puede afectar a las frecuencias naturales y a sus modos normales asociados. Por tanto, es necesario caracterizar el comportamiento de contacto en términos de rigidez y de amortiguamiento asociado a las fuerzas de fricción. Para hacerlo, normalmente se usan tres parámetros: la rigidez de contacto normal, la rigidez de contacto tangencial y el coeficiente de fricción entre las superficies.

En este proyecto, se investigará un método para estimar la rigidez de contacto entre dos golpes planos con bordes redondeados. Para ello, se realizarán simulaciones numéricas usando Ansys, que usa un análisis de elementos finitos y soluciones de ecuaciones no lineares, ya que usará elementos de contacto para caracterizar la zona de contacto. Como consecuencia, se definirá un solucionador de ecuaciones y un método de solución.

A continuación, se obtendrá la rigidez de la articulación caracterizada por un golpe plano, primero aplicando solo un desplazamiento normal a la superficie superior del golpe plano para calcular la rigidez normal de contacto equivalente y a continuación se le añadirá fricción y un desplazamiento normal y tangencial en el mismo lugar para evaluar la rigidez tangencial. Se prestará especial atención a si los resultados numéricos dependen del mallado. Por tanto, se detallará una manera de definir la rigidez de contacto que sea independiente del mallado para encontrar el patrón que la rigidez local de la articulación (afectada por las propiedades del material y por la geometría del golpe plano) sigue a lo largo del cuerpo. En detalle, la rigidez será menor cerca de la superficie de contacto debido a la geometría específica del golpe plano: para una fuerza dada, los desplazamientos relativos, y en consecuencia la deformación elástica, serán mayores cerca de la zona de contacto.

Title: Study of a simplified friction joint for the identification of the contact stiffness

Author: Irene Rodríguez Gauxachs

Directors: Christian Maria Firrone, Jose Ignacio Rojas Gregorio

Date: July 17, 2020

Overview

Turbine blades normally use mechanical joints to attach themselves to turbine disks. In this kind of joints, contact problems are very common. They are called contact problems because they occur where two localized surfaces are in contact. In these cases, peculiar behaviours with respect to the global behaviour of the structure due to high stresses and friction-related effects occur. In some cases, the specific contact behaviour can affect the global behaviour of the structure and it cannot be neglected: from the static point view possible stress intensifications can lead to failure, while from the dynamic point of view the joint may act as a constraint. Therefore, the contact might affect natural frequencies of the structure and associated normal modes. Thus, it is necessary to characterize the contact behaviour in terms of stiffness and damping associated to friction forces. To do so, usually three parameters are used: the normal contact stiffness, the tangential contact stiffness, and the friction coefficient between the surfaces.

In this project, a method to estimate the contact stiffness between two flat punches with rounded edges is investigated. To do so, numerical simulations will be performed using Ansys, using the finite element analysis (FEA) and the solution of non-linear equations since contact elements are used. As a consequence, a numerical equation solver and a solution method will be defined.

To perform a numerical simulation, the finite element is defined in Ansys using a parametric construction of the model. The model will be meshed to obtain more precise results in specific areas close to the contact, but the mesh might affect the results of the contact simulation when a preload is applied. Therefore, before obtaining contact stiffness results, a mesh validation study will be developed comparing the numerical and analytical results for normal pressure distribution of a specific geometry to select the adequate mesh that will provide robust numerical results similar to the ones obtained with the analytical formulation. Then, the stiffness of the joint characterized by a flat punch will be obtained, first applying only a normal displacement to the top surface of the flat punch to calculate an equivalent normal contact stiffness and then applying a normal and a tangential displacement in the same location to calculate an equivalent tangential contact stiffness. Attention to the results is paid if the

numerical results depend on the mesh (mesh-dependency). Therefore, a way to define a contact stiffness that is mesh-independent will be provided in order to find the pattern that the local stiffness of the joint (affected by the material property and the geometry of the punch) follows along the body. In detail, it will result smaller near the contact surface because of the specific geometry of the flat punch geometry: for a given force, the relative displacements and therefore the elastic strain will be larger close to the contact surface.

To Christian M. Firrone,
without whose help this project would have been impossible.

To Anna, Joan and Jose,
for being a huge moral support.

CONTENTS

LIST OF FIGURES

LIST OF TABLES

CHAPTER 1. Introduction

1.1 Stiffness in contact areas

Contact problems are very common in engineering, especially in mechanical joints of turbine blades used in aeronautics, for example, in the dovetail attachment used in a jet engine to attach blades to disks (see Fig. 1.1). Dovetail joints are widely used in aeronautics for attaching blades into compressors or turbine disks.

Contact problems are also found in another kind of joints as in the vane segment that uses two frictions joints: interlocking and the hooks (see Fig. 1.2) used to connect the structure of a stator vane segment to the corresponding casing sector. Contact problems are also present in blade shrouds (see Fig. 1.3) where the turbine blades have T-shaped tips that touch each other to form a ring to support the blades around the turbine wheel.

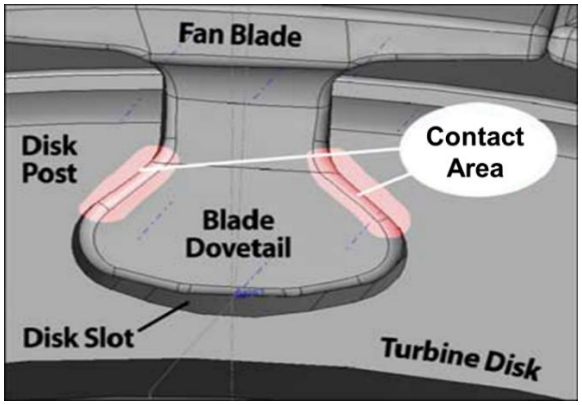

Fig. 1.1 Sketch of a dovetail blade into a turbine disk [1]

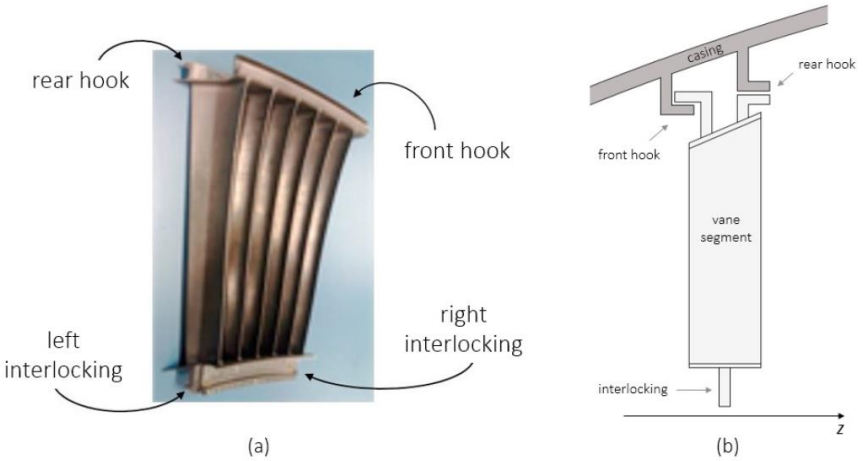

Fig. 1.2 (a) Real vane segment of a low pressure turbine module for aeronautical applications; (b) schematic view of a stator vane segment connected at the casing by means of hook joints [2]

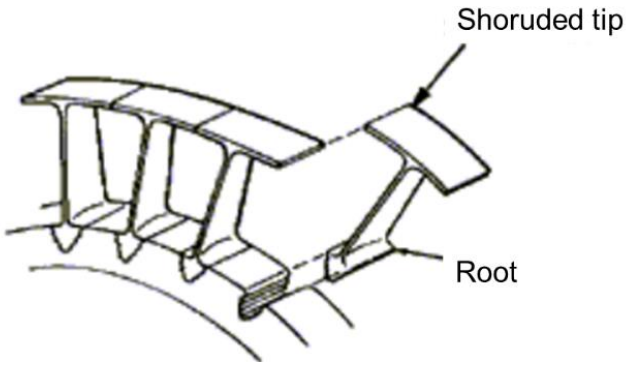

Fig. 1.3 Sketch of a blade shroud tip [3]

Joints are used mainly to connect components between them, but they are also used to produce friction forces in order to dissipate energy of the whole structure and, consequently, the structure will have smaller vibrations. Many of these friction joints use a flat contact to optimize friction, as can be seen in the previous figures. Therefore, the flat punch geometry will be studied in this project.

It is important to predict the fatigue and possible failures of the structure due to the contact problem by studying the resonance frequencies and the forced response levels to anticipate the behaviour of the joint. For example, in a dovetail joint, as the turbine disk rotates, the stress in the contact area will increase, achieving really high stresses that cannot be neglected.

Thus, it is necessary to characterize the contact behaviour in terms of stiffness and damping associated to friction forces. An accurate contact modelling requires the knowledge of mainly three parameters to characterize the contact behaviour: the normal contact stiffness, the tangential contact stiffness, and the friction coefficient between the surfaces.

Unfortunately, contact problems cannot be solved normally by classical methods (for example, analytical methods) because they usually involve very complex configurations. Nowadays, these kind of problems are solved using numerical methods and finite element analysis (FEA), for instance using Ansys.

1.2 Objectives

The main objective of this project is to provide a simple and effective method to estimate the contact stiffness between two flat punches with rounded edges. This geometry has been selected because it is a simplification of a joint geometry widely used in aeronautics that uses a flat contact to decrease friction effects (see Fig. 1.1 to Fig. 1.3). To do so, numerical results will be obtained from simulations using Ansys. For this purpose, we will use Ansys Parametric Design Language (APDL) and a mesh for the studied geometry. Another main objective would be to remark the importance of a refined mesh used in the contact model to obtain mesh-independent results and, consequently, robust.

In order to achieve these objectives, the following topics have been addressed:

- Defining contact models using the parametric design of Ansys Mechanical APDL.
- Using Ansys Mechanical APDL as a tool to perform simulations in mechanical problems, getting familiar with his graphic interface and exploring the post-processing options.
- Creating various MATLAB codes to process the results obtained with Ansys simulations.

1.3 Project structure

The project will be structured in six chapters:

- First of all, with CHAPTER 1, the difficulty of studying the contact stiffness is captured, as well as the importance of a refined mesh in any simulation. In addition, the objectives and project structure are defined.

- Secondly, in CHAPTER 2, Ansys Mechanical APDL is introduced. This will be the program used to perform all the simulations. Specifically, this chapter will explain what tools Ansys uses for defining a finite model and to solve a contact problem.

- Then, in CHAPTER 3, the mesh validation is performed. This means that a mesh will be defined as refined enough for obtaining the results of the contact stiffness numerically, with acceptable accuracy and resolution at an acceptable computational time. The mesh will be chosen if, when comparing the pressure distribution results, it is found that the analytical and numerical the results are very similar.

- After that, in CHAPTER 4, the normal contact problem will be defined in order to find the pattern that the stiffness follows through the body when a normal displacement is applied in the upper surface.

- To continue, in CHAPTER 5, a normal and tangential displacement and friction between the surfaces will be introduced. The differences with the previous results will be discussed.

- To conclude, in CHAPTER 6, the conclusions of the project comparing the results of the numerical simulations are exposed and also some future work is proposed.

CHAPTER 2. Ansys Mechanical APDL

Ansys Mechanical APDL is the program used to obtain the numerical results with the different contact models. Particularly, the models will be defined using APDL and contact elements. The problem will be solved using non-linear equations. In consequence, a numerical equation solver and a solution method will be defined.

It is important to remark that all the data (displacements, forces, pressure) will be obtained in the nodes of the finite elements. In Ansys, a node can be defined as a coordinate location where the degrees of freedom (DOFs) are designated. The DOFs also represent which moments and forces are transferred from one node to the next one. The nodes also delimitate the cells of the mesh. Therefore, if the mesh has smaller elements, the nodes density will be higher.

2.1 Finite Element Analysis (FEA)

APDL is a scripting language used in Ansys. All operations that can be done using the graphical user interface (GUI) can also be performed by writing down commands using APDL. Specifically, PREP7 Commands are used to create and set up the model [4]. They are written in a .txt file and imported to Ansys as an input to create the finite element. In this way, it is easier to make changes in the geometry of the figure, the mesh, or the boundary conditions. The rest of operations such as solving the problem or post-processing the model are done with Ansys GUI.

The typical steps followed by Ansys in FEA are shown in Fig. 2.1 .

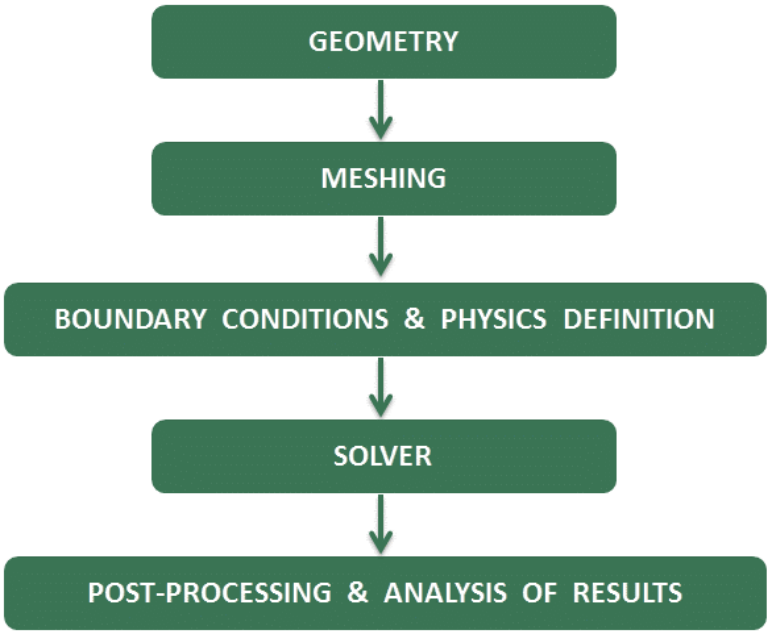

Fig. 2.1 Steps of numerical analysis in finite element analysis (FEA)

To begin, in order to define the geometry for a finite element, several steps must be followed:

1. First of all, the element type and the material properties (Young's modulus, Poisson ratio and density) are defined.
2. Then, to start building up the body, the key points are defined. These key points will be connected by lines, and in turn, lines will create areas in the same way.

To continue, in order to define the mesh, the lines are divided depending on the number of elements needed for each line. They can use a ratio to have different sizes of elements along the same line. For example, a ratio can be used to have small elements near the area of interest and larger elements where such level of accuracy is not needed. After that, the mesh can be created along the geometry. When the body is meshed, a volume is generated for each area to have a 3D body and the divisions of elements along the thickness will be defined as well.

Then, the boundary conditions are defined, which means that nodes are grouped into components and constraints and/or contact elements are assigned to the nodes components to make the finite element resemble the physical phenomenon.

To continue, a numerical solver that uses the Newton-Raphson iterative method is used to find a solution. And, to conclude, with Ansys Mechanical APDL but also with MATLAB, the results are post-processed and analysed to obtain a significant solution.

An example of a finite element defined using parametric design to set up the model can be seen in APPENDIX A, where the geometry, the mesh, and the boundary conditions are defined.

2.1.1 Influence of the mesh quality on the results

One of the most important factors when a simulation is made with any application that uses FEA is the mesh of the geometry to be simulated. The mesh quality plays a main role in the stability and precision of the numerical calculations. When a model is meshed, a medium that is actually continuous is discretized, and the degree of accuracy and resolution that will be achieved in the most complex zones will depend on the density and the distribution of nodes of the mesh in that area.

To select a correct mesh, it is important to check some parameters such as the time necessary to create the mesh and the computational cost of the simulations. Most of the geometries studied in simulations are complex and therefore their meshes will be complex to design as well.

A mesh can be defined with tetrahedral or hexahedral cells. On the one hand, the tetrahedral mesh is used for more complex geometries because it allows the cells to be grouped in the regions selected and the hexahedral ones can require many

cells in zones where they are not needed. On the other hand, tetrahedral meshes allow best appearance relations, this means with angles close to 90º and with an appearance relation smaller than 5:1 [5].

In a three-dimensional (3D) problem, there is more conditioning of the CPU and the computer memory used to perform the simulation. As it is to expect, the higher accuracy will be obtained with more refined meshes but with the cost of higher calculation and postprocessing times of the solution so there has to be a trade-off between both parameters to archive and acceptable solution.

2.2 Contact elements

To solve a contact problem between two solids, Ansys uses Contact elements. These are used mainly to compute stresses at the contact area. There are different approaches [6]: point-to-surface, surface-to-surface, node-to-surface or node-to-node using one of five possible contact algorithms that will be discussed in Section 2.3. Depending on the circumstances, one of the options will be better than the others.

In this project, node-to-node contact elements will be used. These type of contact elements are used when the location of the contact is known beforehand. In the problem, the contact surface will be defined as the flat punch and the potential contact surface with the aim of covering all the possible contact surface. Besides, node-to-node contact elements allows extremely precise analyses of surface stresses, one of the most interesting parameters to study in this project (see CHAPTER 3).

In each contact area, a contact pair will be defined: one surface will be the *Contact surface* and the other one the *Target surface*, with the former surface moving into the latter surface. In a contact pair, to have the contact area resembles reality with a fast convergence of the solution, the following concepts must also be defined:

- The friction coefficient between the contact areas
- If the contact includes initial penetration between the bodies
- Contact properties, such as penetration tolerance between the bodies
- Solution algorithm

If a same numerical solution is obtained from simulations of the problem using different solutions algorithms and/or different element types, and this solution has a physical sense, it is considered to be a robust solution.

2.3 Solution algorithms

As said in the previous section (see Section 2.2), when a contact pair is defined a solution algorithm must be defined. These algorithms use a non-linear calculation process to find the solution.

There are four solution algorithm and each one requires different predefined parameters [7]:

- Pure Lagrange multiplier method: Ensures no penetrations between the elements and compressive contact force and pressure. In this case, the parameters to be defined are:
  - TOLN: maximum allowable penetration tolerance
  - FTOL: maximum allowable tensile contact pressure

- Lagrange multiplier method: Maximizes the elastic tangential force minimizing the displacement. In this case, the parameters to be defined are:
  - STOL: maximum allowable elastic slip
  - FKS: tangent penalty stiffness

- Augmented Lagrange method: Minimizes the penetration with a robust convergence. In this case, the parameters to be defined are:
  - FKS
  - TOLN
  - STOL

- Pure penalty method: Find the equilibrium between the forces. In this case, the parameters to be defined are:
  - FKS
  - FKN: normal penalty stiffness

The most common methods are the Pure Lagrange multiplier method and the Penalty method [8]. The remaining ones are considered to be intermediate methods between the previous two because the parameters they need are similar to the ones used in the main solution methods.

In our study, the Pure Lagrange multiplier method will be used. It is the solution algorithm that most resembles the physical phenomenon studied in this project since in the other cases some penalty stiffness (FKS and FKN) is introduced to have a conversion of the solution, ergo they introduce some numerical parameters in order to have a faster conversion of the solution but this will interfere with the results obtained. Therefore, the solution of the stiffness obtained would be modified by the penalty stiffness previously defined. Hence, the only method that does not introduce some penalty is the Pure Lagrange multiplier.

2.4 Newton-Raphson numerical method

The solution algorithms defined in the previous section (see Section 2.3) use a non-linear calculation to find the solution; particular, they use the Newton-Raphson numerical method that follows an iterative procedure [9]. This means that several iterations are made until the solution converges.

The Newton-Raphson method is based on linear approximation. If $f(x)$ is a function with root r, at the beginning an x_o is provided as a tentative solution and the error between the tentative solution and the real root is evaluated. Then, x_1 is obtained as an improved solution of x_o because it will have a smaller error. This procedure can be repeated iteratively: x_2 will be defined as an improved solution of x_1 and so on. The next solution in each iterative step is calculated as:

$$x_{i+1} = x_i - \frac{f(x_i)}{f'(x_i)} \tag{2.1}$$

This method can be seen more clearly in the graphic in Fig. 2.2 more clearly:

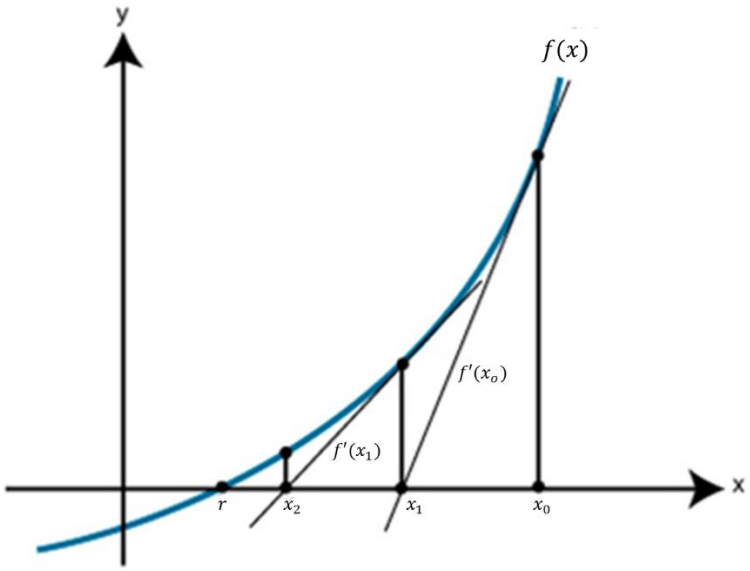

Fig. 2.2 Newton-Raphson method in successive iterations

The solutions in each iterative step are said to be improved because they are considered to be closer to r. For that reason, a new parameter must be defined: the residual (res).

$$res = x_i - r \tag{2.2}$$

If the residual is very small, it means that the tentative solution is close to the root. As the residual gets smaller, the solution will be closer to the correct one. Ideally, the iterations could be performed until the residual is zero, but this would significate a very high computational effort, both in computational time and memory. That is why the residual is considered to be good enough if it is smaller than a given tolerance.

Normally, the simulation results should converge as the number of iterations increases, which means that the difference between the residual and the tolerance should be smaller as the iterations increase.

CHAPTER 3. Mesh validation

As said in Section 2.1.1, the mesh quality is the basis of any simulation. Hence, it is essential to define a good mesh in Ansys to find an accurate result for contact stiffness. Therefore, it is necessary to check the results obtained from theoretical and/or experimental approaches to validate the results obtained numerically from the simulations. For that purpose, the numerical result of the contact pressure distribution is the parameter chosen to be compared with the analytical results because it can be obtained easily using Shtayerman's work [10].

If the mesh is refined enough, the numerical results will be very similar to the analytical ones and we will be able to affirm that the results are mesh-independent and therefore robust. Then, this contact model can be used to calculate contact stiffness.

3.1 Contact model and boundary conditions

In this section, the contact model used to validate the mesh and its boundary conditions are explained.

The problem to be studied is 3D: a prism with smoothed edges at contact on top of a semi-infinite plane. Fig. 3.1 and Fig. 3.2 show the geometry and the reference frame used, front and oblique views, respectively. The flat punch of the model can be distinguished with a red line.

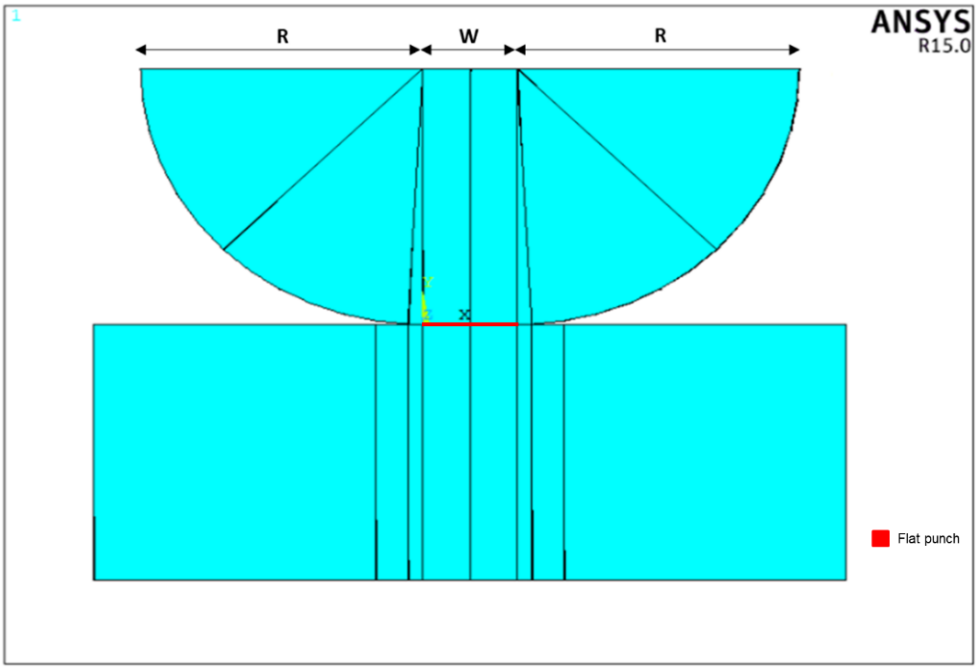

Fig. 3.1 Contact model geometry for mesh validation (front view, showing the reference frame used in this work)

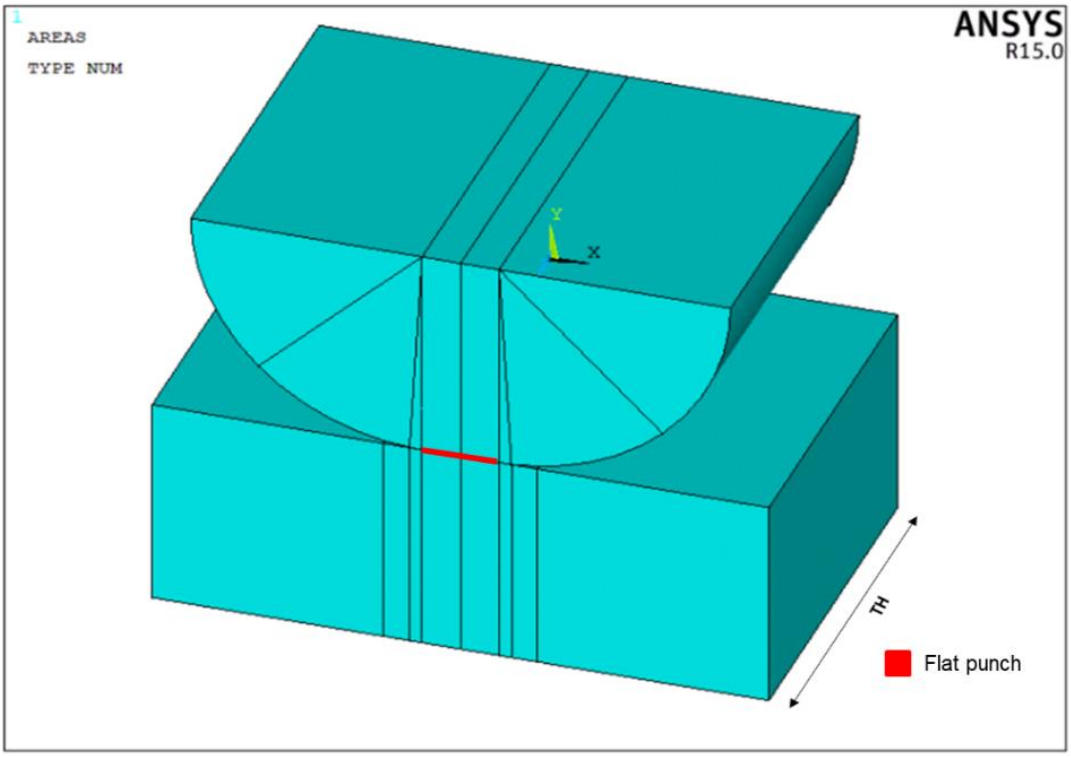

Fig. 3.2 Contact model geometry for mesh validation (oblique view, showing the reference frame used in this work)

As can be seen in the previous figures, the thickness (*TH*) is larger than the width (*w*). The geometry was designed in this way to avoid the unrealistic alterations of the numerical results close to the sharp change of geometry, due to the change of geometry itself. This edge effect is due to the strong discontinuity of the geometry that does not exist in reality, but it is a limitation of the model for the simulation. This discontinuity may cause a strong variation of boundary conditions, which may affect the obtained numerical results, such that they would be far from the real physical behaviour.

The boundary conditions are defined by the constraints applied to the bodies. In this case, on one hand, the lower body is constrained; hence, the nodes have of the bottom surface of the lower body have no displacement in any direction. On the other hand, the upper body has a normal displacement applied on the top surface (*Uy*). This displacement will cause a reaction force per unit length (*P*) on the bottom surface of the lower body, as it can be seen in Fig. 3.3 .

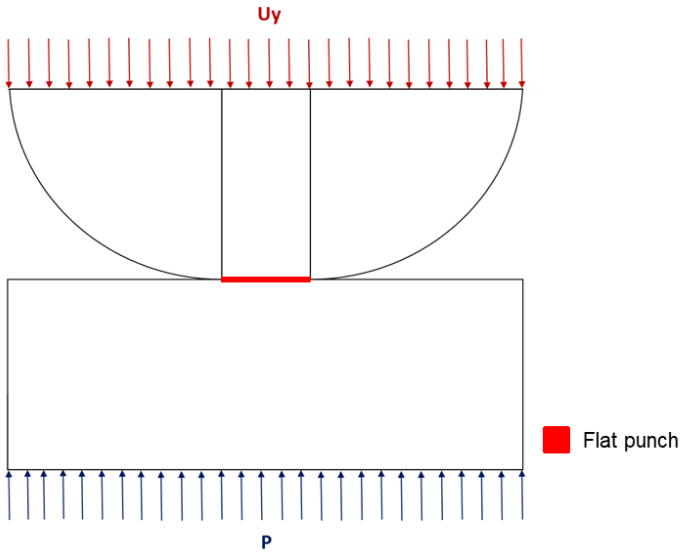

Fig. 3.3 Sketch of the normal displacement (*Uy*) and the reaction force (*P*) in the top surface of the upper body and the bottom surface of the lower body, respectively

Notice that Fig. 3.3 is a two-dimensional (2D) sketch of the cross section. Nevertheless, *Uy* and *P* are applied along the all the thickness (third dimension, normal to the cross section) in the upper and bottom surfaces.

Contact elements are defined in the contact area, mainly in the flat punch. In this case, contact elements will have no initial penetration and no friction between surfaces will be applied. Furthermore, as said in Section 2.3, Pure Lagrange Method will be used as the solution algorithm.

The material chosen is steel because joints used in aeronautical engines are mainly made of this material. The displacement and dimensions of the model have been chosen arbitrarily, just to find a meaningful result.

The parameters used in this contact model can be seen in Table 3.1.

Table 3.1. Values of the parameters used for the mesh validation

Parameter	Value	Units
Normal displacement (*Uy*)	-25	μm
Radius of curvature (*R*)	4650	μm
Width of the flat punch (*w*)	1550	μm
Thickness (*TH*)	7750	μm
Young's modulus (*E*)	205	GPa
Poisson ratio (*v*)	0.3	-

The simulations of all this study have been performed with a computer processor Inter® Core™ i5 CPU M 540 @ 2.53GHz and with a RAM of 8 GB. The simulations' solutions take between 10 to 50 minutes to converge, depending on the number of cells of the mesh used.

3.2 Mesh independence study

As said in Section 2.1.1, the main idea of a mesh is to have smaller elements (that is, a finer mesh) closer to the studied contact area, especially in the edges, to have more accurate results in that area, and larger elements (that is, a coarser mesh) on the rest of the body to decrease the computational costs. In this chapter, a mesh independence study is conducted, and for this purpose, three types of mesh will be analysed to see the impact of the mesh on the numerical results. Each one will have a different number of elements and sizes of elements.

For defining a mesh, it is necessary to make divisions of the lines that define the body to create the cells. In this way, if there are many divisions along a line, the mesh will have very small elements. Not all the lines that define the geometry must be divided into the same number of elements. It is best to have a more refined mesh near the contact area and a mesh with larger elements in areas that are far from the contact area. In this way, a trade-off solution is obtained with the result in the contact area being accurate, while the computation time decreases significantly.

In this contact model, the lines of the body can be grouped into 5 different types depending on the number of divisions of each of them as it can be seen in Fig. 3.4 .

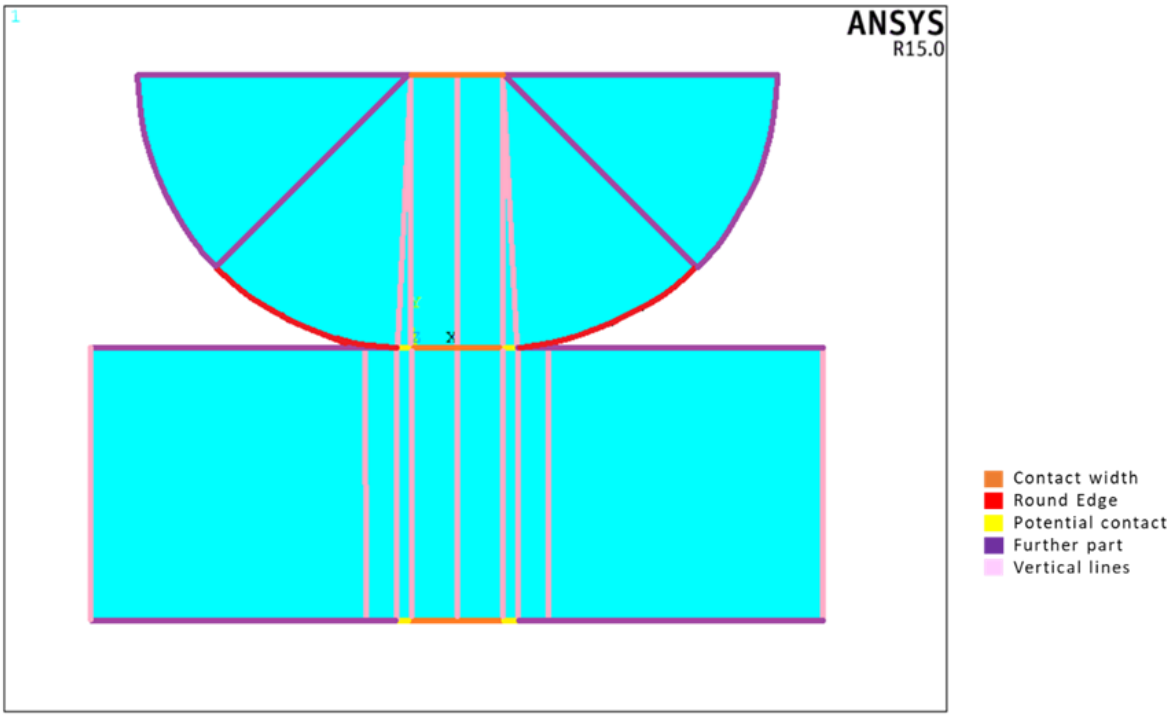

Fig. 3.4 Types of lines in this study depending on the number of divisions in the line for defining the mesh

For each mesh, each of the types of lines will have a different number of divisions and therefore, mesh cells as shown in Table 3.2.

Table 3.2. Number of elements in each of the types of lines for each of the studied meshes in the mesh validation study

Mesh	Contact width	Round edge	Potential contact area	Further part	Vertical lines	Total number of cells
1	20	12	25	20	20	52910
2	30	25	50	12	50	120654
3	30 (40)	25 (4)	60 (10)	12	60 (100)	146992

As can be seen in the previous table, the most refined mesh is mesh 3 because it is the one with a higher number of cells in all geometry. It is also the mesh that has more cells near the contact area, that will be defined as the contact width and potential contact area. Notice that the number of elements along the lines of the further parts has been decreased to have a reasonable computational time while increasing the elements of the most significant lines.

Between parentheses, it is indicated the ratio used so not all the elements along the line have the same size. For example, a ratio of 40 will mean that the biggest element is forty times the smallest element. This is useful to have even smaller elements near the contact area without increasing the computation time.

The three different meshes used in this study can be seen in detail in the next figures. Fig. 3.5 and Fig. 3.6 show mesh 1, Fig. 3.7 and Fig. 3.8 show mesh 2 and finally Fig. 3.9 and Fig. 3.10 shown mesh 3.

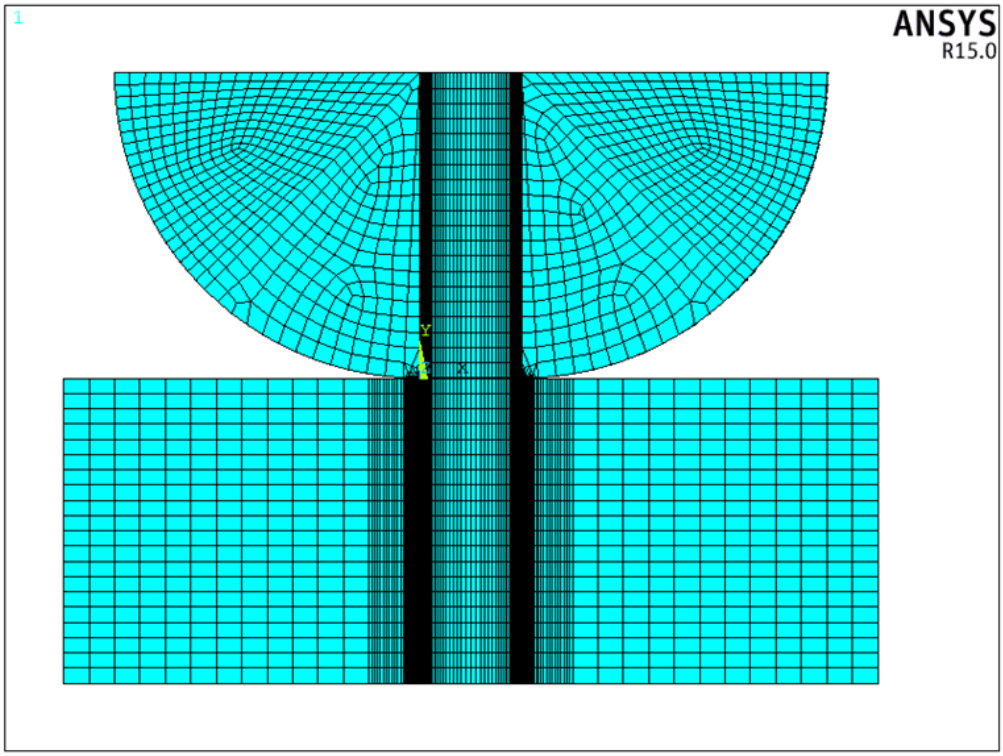

Fig. 3.5 Front view of mesh 1 (20 elements along the major vertical axis)

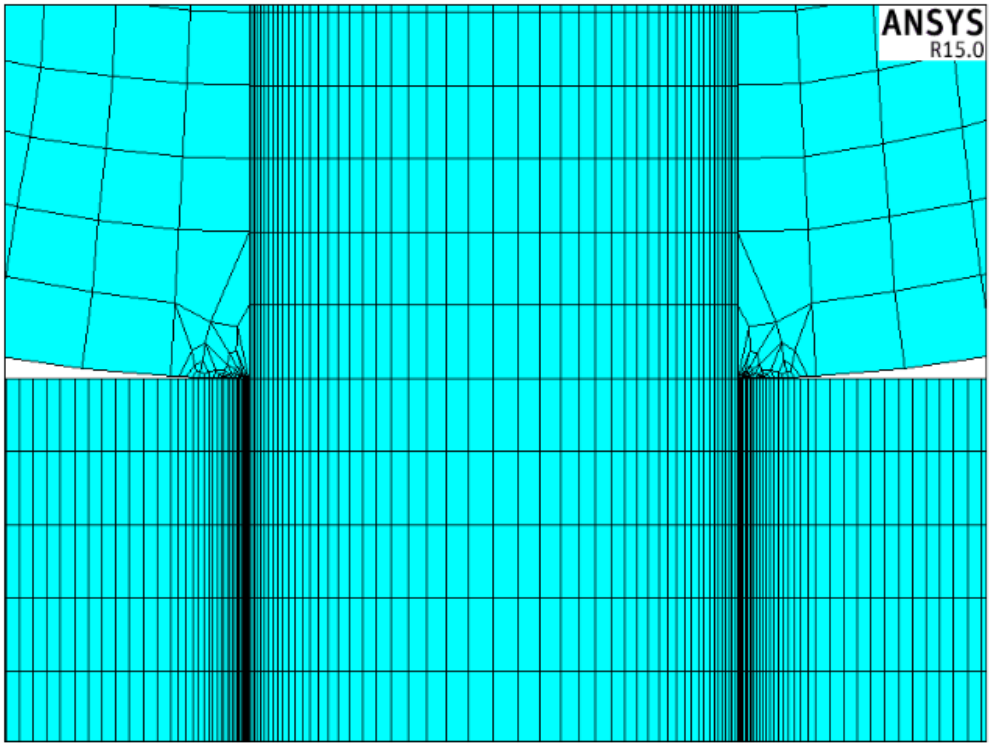

Fig. 3.6 Detail front view of mesh 1 near the contact area

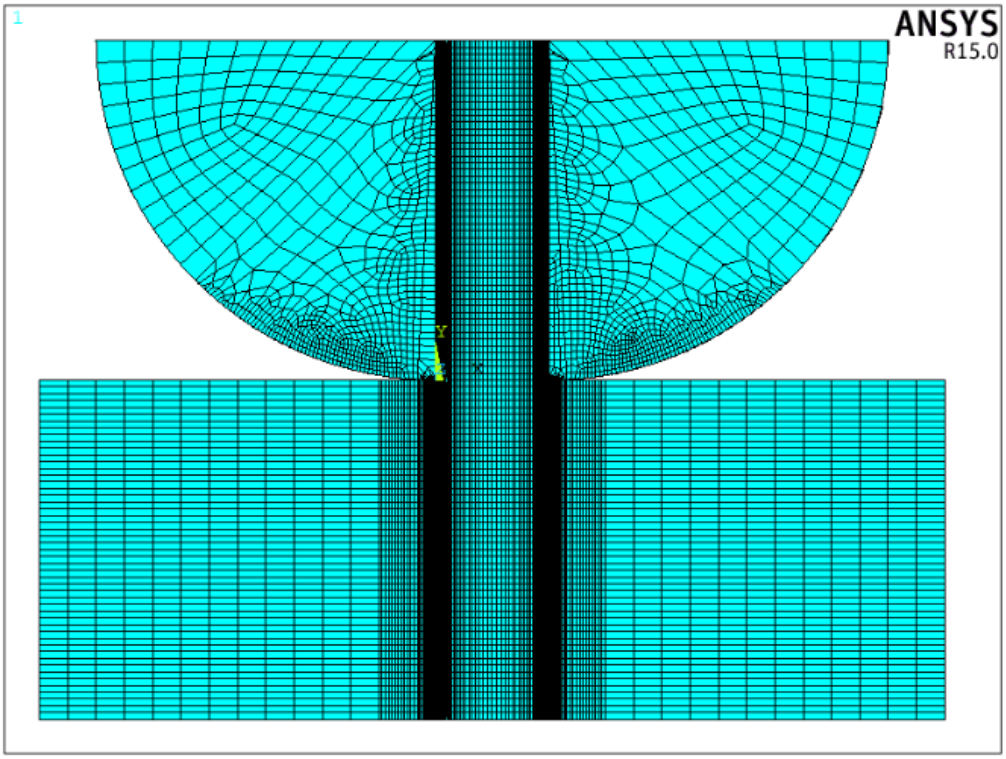

Fig. 3.7 Front view of mesh 2 (50 elements along the major vertical axis)

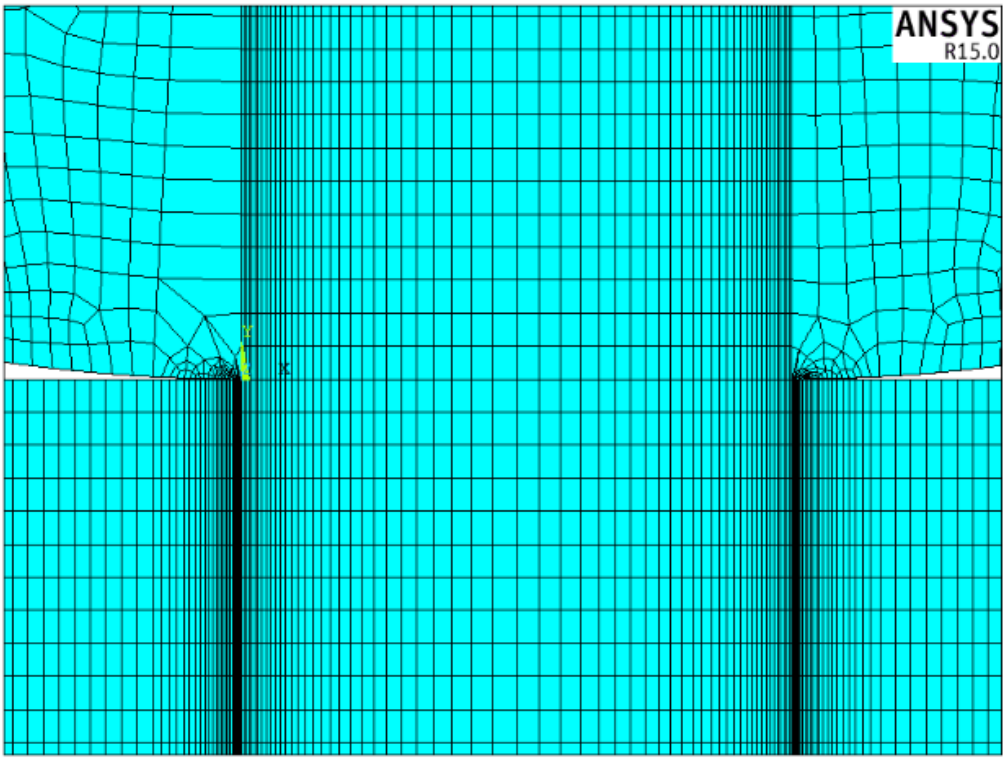

Fig. 3.8 Detail front view of mesh 2 near the contact area

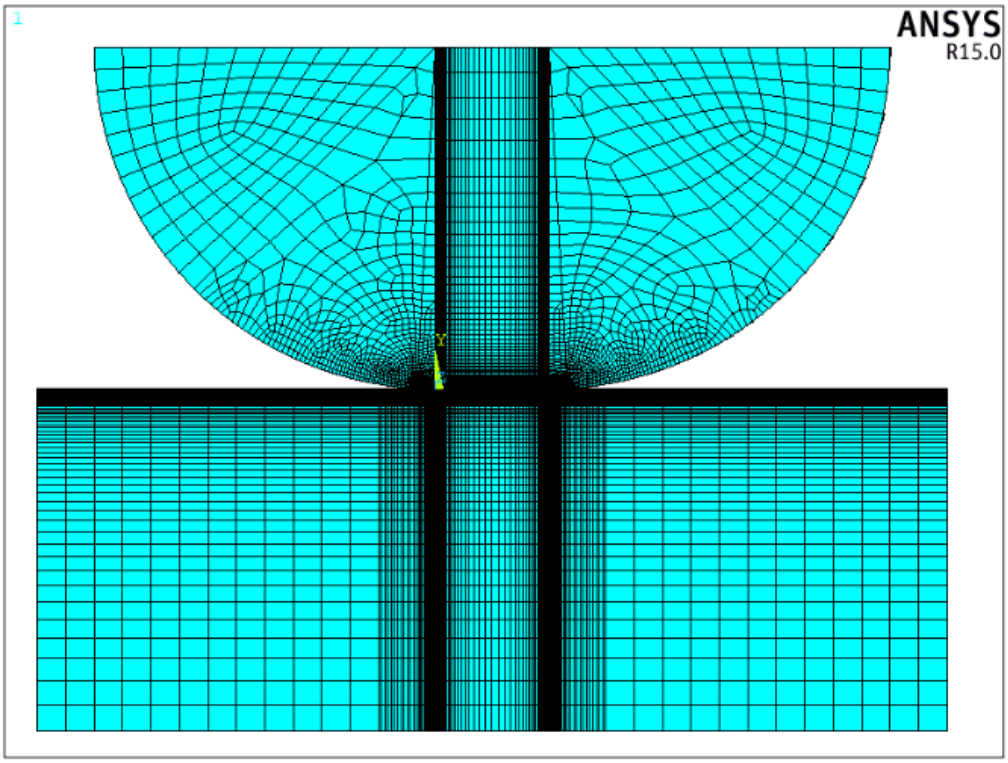

Fig. 3.9 Front view of mesh 3 (60 elements along the major vertical axis with ratio)

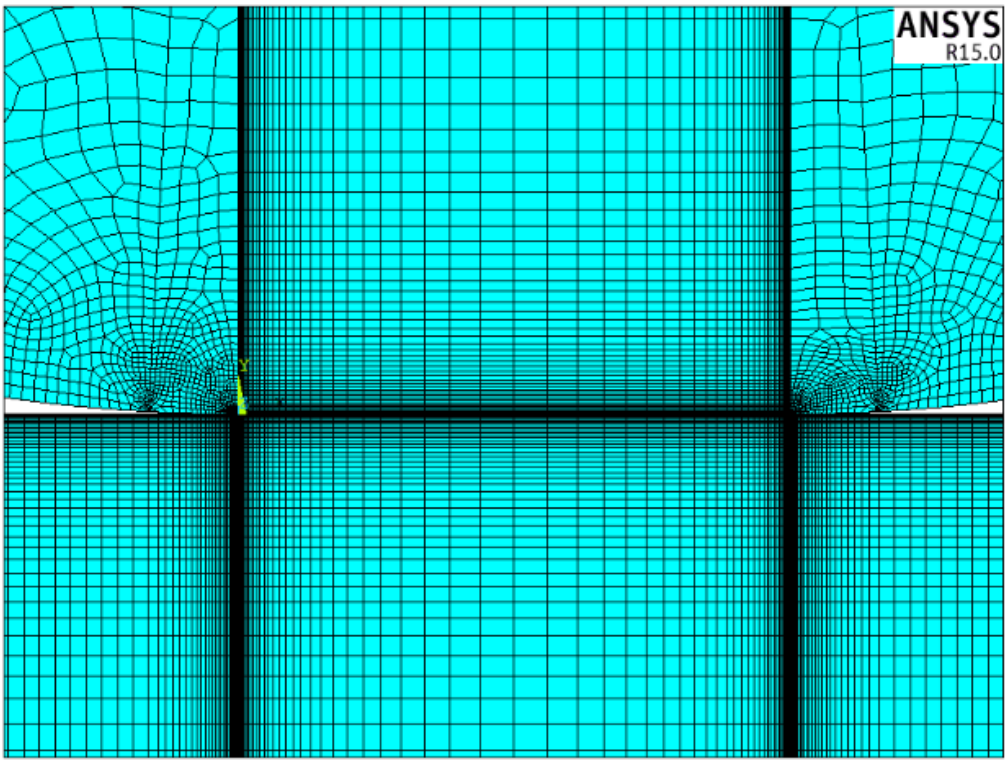

Fig. 3.10 Detail front view of mesh 3 near the contact area

3.3 Analytical results

First, the analytical results of the pressure distribution must be obtained and then they will be compared with the numerical results from the simulation.

Analytical solutions for the 3D problems do not exist or they are really difficult to achieve and/or are only valid in a very few simple cases. However, there are several studies of analytical solutions for a 2D problem. In our case, a 2D model by Shtayerman has been used as reference [10].

Shtayerman model's states that, for a flat punch with rounded edges on top of a semi-infinite plane, the pressure distribution $p(x)$ depends only on the ratio a/b where a is the half width of the flat punch ($a = w/2$), which is known, and b is the half width of the contact area after the load is applied, which is unknown. The a/b ratio can be found with the next equation.

$$\frac{2PR}{a^2E^*} = \frac{\pi - 2\varphi_0}{2\sin^2\varphi_0} - \cot\varphi_0 \qquad \textbf{(3.1)}$$

where P is the applied normal force per unit length, R is the radius and $\sin\varphi_0 = a/b$. E^* measures the combined of the stiffness of the two bodies and can be defined with the equation 3.2.

$$\frac{1}{E^*} = \frac{1}{E_1}(1 - {v_1}^2) + \frac{1}{E_2}(1 - {v_2}^2) \quad \textbf{(3.2)}$$

where E is the Young's modulus and v the Poisson ratio. In this contact model, both are the same for both bodies because they are made of the same material with the same mechanical properties so the equation can be written as:

$$\frac{1}{E^*} = \frac{2}{E}(1 - v^2) \quad \textbf{(3.3)}$$

The equation 3.1 is solved with numerical methods to find φ_0 and therefore a/b.

The normal pressure distribution $p(\varphi)$ is provided by the next equation.

$$p(\varphi) = \frac{P}{b} f(\varphi_0, \varphi) \quad \textbf{(3.4)}$$

where $\sin\varphi = x/b$ and $f(\varphi_0, \varphi)$ is defined as:

$$f(\varphi_0, \varphi) = \frac{2/\pi}{\pi - 2\varphi_0 - \sin 2\varphi_0}\left\{(\pi - 2\varphi_0)\cos\varphi + ln\left[\left|\frac{\sin(\varphi+\varphi_0)}{\sin(\varphi-\varphi_0)}\right|^{\sin\varphi}\left|\tan\frac{\varphi+\varphi_0}{2}\tan\frac{\varphi-\varphi_0}{2}\right|^{\sin\varphi_0}\right]\right\} \quad \textbf{(3.5)}$$

Finally, taking the parameters P, R, w, E and v as known, the pressure distribution is defined applying the previous formulas in a MATLAB code (see Appendix B.1).

As an example, a value of P will be assigned to this simulation to show the pressure distribution. In this case, the value assigned for P is 2028 kN/m.

The contact pressure distribution obtained along the X axis of the contact surface can be seen in Fig. 3.11 . As can be observed, the pressure distribution is symmetric with respect to the vertical middle axis because the defined contact model is also symmetric. Moreover, the pressure is significantly higher in the edges of the contact surface compared to the central region.

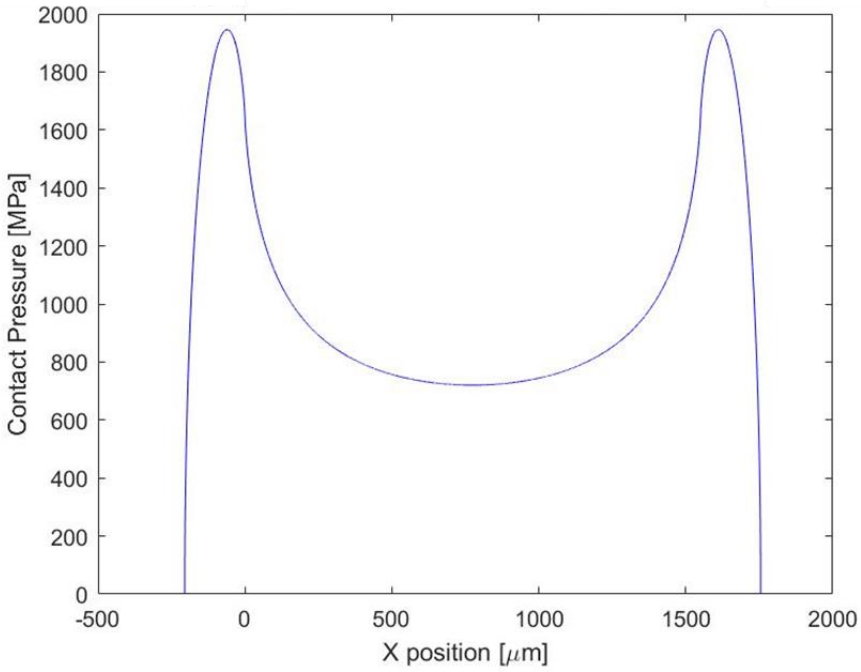

Fig. 3.11 Analytical results for the normal contact pressure distribution

3.4 Numerical results

The second step is to obtain the numerical results of pressure distribution with the contact model defined in Ansys. As said before, the obtained analytical results are for a 2D problem so that thickness is not considered. Our problem and numerical model is 3D; therefore, only a cross section of the body will be considered to compare the results as it can be seen in the next sketch. In this case, only the nodes in the middle plane (that is, all the nodes with a position Z = *TH*/2, as shown in Fig. 3.12) are studied to avoid edge effects.

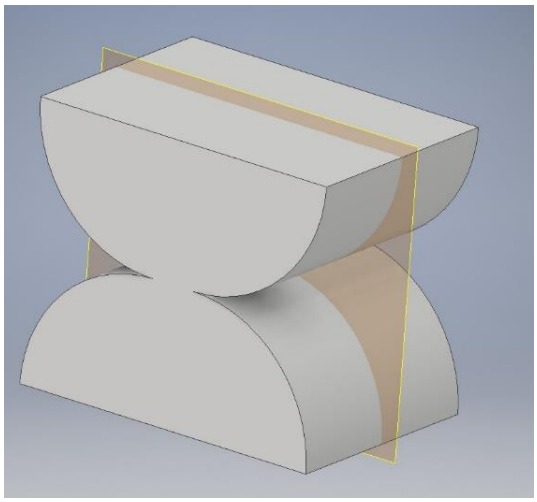

Fig. 3.12 Middle plane of the geometry from which the numerical results are obtained for comparison purposes with the analytical results

Once we obtain the nodes in the contact area in the middle plane and the pressure for each of them, the pressure distribution can be plotted. The numerical results obtained for the different contact models (that is, for meshes 1 to 3) are shown from Fig. 3.13 to Fig. 3.15 .

Notice that the load per unit length (*P*) is not an initial input but a parameter obtained after the simulation because it is the reaction force after applying a displacement. This value will vary depending on the mesh used because each mesh has a different pressure distribution obtained with numerical results. A force can be defined as the integral of the pressure in a surface. Therefore, if the values of the pressure distribution change, the reaction force will change as well.

In Table 3.3, the *P* obtained for each mesh are shown.

Table 3.3. Reaction force per unit length for each mesh in the mesh validation

Mesh	*P* (kN/m)
1	1878.45
2	1871.48
3	2028.39

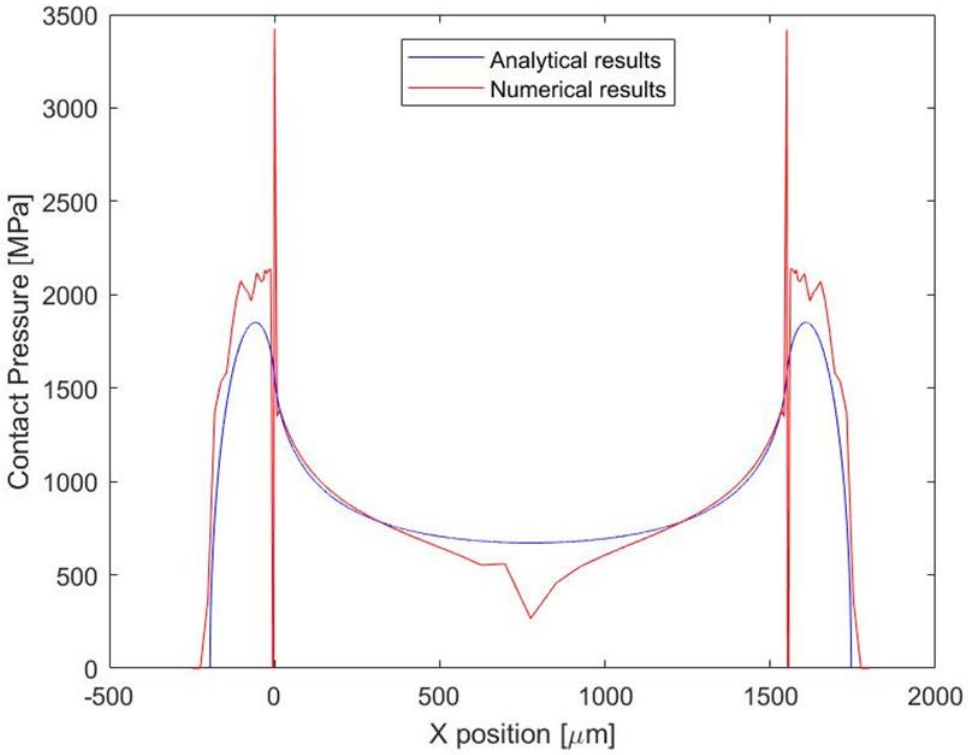

Fig. 3.13 Numerical and analytical results for normal contact pressure distribution for mesh 1

Fig. 3.13 shows the results of the contact pressure distribution for mesh 1. Mesh 1 is the less refined mesh because the cells are bigger in all along the body (that is, a smaller number of total cells) with respect to the other two meshes.

As can be seen in the previous plot, the numerical results are not similar to the analytical results. To study the difference between the analytical and numerical results, the absolute and relative errors have been computed in some key X positions as can be seen in Table 3.4.

Table 3.4. Absolute and relative errors for the pressure distribution of the numerical results of mesh 1 with respect to the analytical results

X Position (µm)	Absolute error (MPa)	Relative error (%)
-100	331.5	19.02
0	1862.0	119.21
500	61	8.65
775	404.7	60.29
1000	94.6	13.68
1550	1854	118.54
1650	241	13.00

The relative errors are between 8% and 120% so the numerical results obtained are not accurate, especially in the edges (x = 0 µm and x = 1550 µm) where there is a relative error of 120% approximately. The difference between analytical and numerical results can be due to the mesh configuration because the mesh is too coursed with respect to the geometry. Therefore, it is expected to obtain better results with the following meshes.

In Fig. 3.14 the numerical and analytical results for normal contact pressure distribution for mesh 2 are shown.

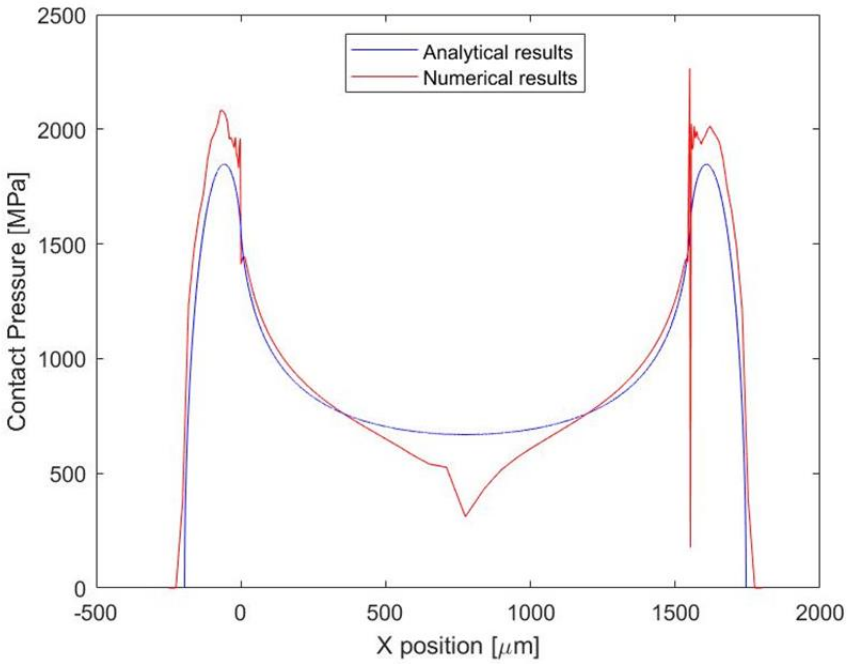

Fig. 3.14 Numerical and analytical results for normal contact pressure distribution for mesh 2

As with the previous mesh, the absolute and relative error have been computed as can be seen in Table 3.5.

Table 3.5. Absolute and relative errors for the pressure distribution of the numerical results of mesh 2 with respect to the analytical results

X Position (µm)	Absolute error (MPa)	Relative error (%)
-100	216.0	12.43
0	146.0	9.37
500	51.6	7.32
775	358.3	53.56
1000	79.9	11.53
1550	703.0	44.98
1650	208	11.99

The relative errors are between 9% and 54% so the numerical results obtained are closer to the analytical results but still, they are not accurate enough. With this mesh, the highest difference is also obtained at the edges where there is a 44% of relative error but also in the central area (x = 775 µm) where there is a relative error of 54%.

In Fig. 3.15 the numerical and analytical results for normal contact pressure distribution for mesh 3 are shown.

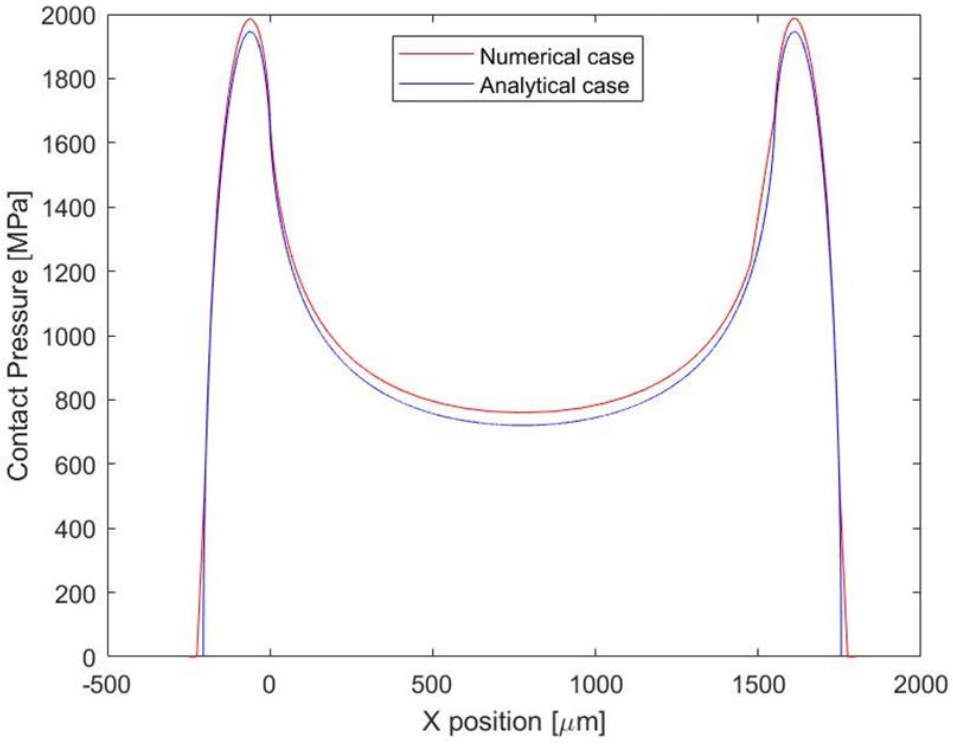

Fig. 3.15 Numerical and analytical results for normal contact pressure distribution for mesh 3

As can be seen in Fig. 3.15 , the results of the mesh 3 are the ones that better match the analytical results, the differences between them are minimal. As with the previous meshes, the absolute and relative error have been computed as can be seen in Table 3.6.

Table 3.6. Absolute and relative errors for the pressure distribution of the numerical results of mesh 3 with respect to the analytical results

X Position (µm)	Absolute error (MPa)	Relative error (%)
-100	40.0	2.16
0	42.0	2.56
500	38.2	5.09
775	39.8	5.53
1000	39.0	5.24
1550	36.0	2.18
1650	40.5	2.17

The relative errors are between 2% and 6% so the numerical results obtained are very close to the analytical results and can be defined as accurate. In this case, the mesh is the most refined because it has the highest number of total cells in the geometry and it is the mesh that has smaller elements near the contact area.

It is concluded that the size of the elements used are sufficient to describe the physical phenomenon and, consequently, the contact model with mesh 3 is the one used to find all the parameters in the contact area in the study from now on.

CHAPTER 4: Normal contact problem

In this chapter, a pattern for defining the contact stiffness when only a normal force is applied will be found.

4.1 Contact model and boundary conditions

The contact model and boundary conditions used in this study are the same as those used for the mesh validation (see Section 3.1). In this case though, we use a prism with smoothed edges on top of another prism with smoothed edges, instead of the semi-infinite plane used in the mesh validation study. The geometry of this contact model, front and oblique views, can be seen in Fig. 4.1 and Fig. 4.2 , respectively.

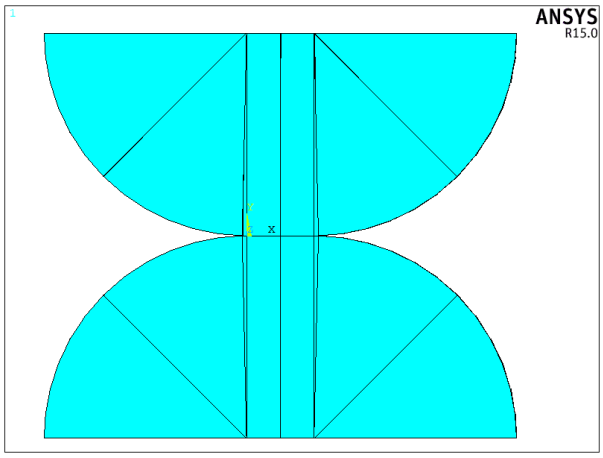

Fig. 4.1 Contact model geometry of the normal contact problem (front view)

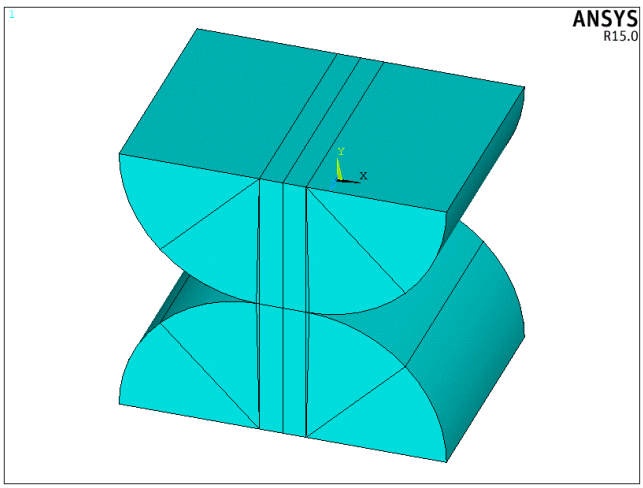

Fig. 4.2 Contact model geometry of the normal contact problem (oblique view)

Table 4.1 shows the values of some of the parameters used in this study, which are the same as those used in the mesh validation study (see Section 3.1) because the same material, geometry, and dimensions are used, with the only exception of the displacement, which is going to be -1 μm. Consequently, the reaction force will change as well.

Table 4.1. Values of the parameters used in the normal contact problem, where normal displacement is applied in the upper surface

Parameter	Value	Units
Normal displacement (*Uy*)	-1	μm
Radius of curvature (*R*)	4650	μm
Width of the flat punch (*w*)	1550	μm
Thickness (*TH*)	7750	μm
Young's modulus (*E*)	205	GPa
Poisson ratio (*v*)	0.3	-

4.2 Normal contact stiffness definition

Stiffness indicates how rigid or flexible a body is. If a normal force is applied upon a body, it will have a larger strain if it is more flexible and a smaller strain if it is more rigid. Therefore, stiffness can be defined as the capacity of a body to resist deformation when a force is applied. This can also be expressed with the next formula when a normal force or displacement is applied upon the body.

$$k_N = \frac{F_N}{u_{rel\,N}} \tag{4.1}$$

where F_N is the applied normal force, k_N is the normal stiffness and $u_{rel\,N}$ is the normal relative displacement.

In this problem, the relative displacement will be computed as the difference between the displacement of two consecutive nodes as shown in the following equation.

$$u_{rel} = u_{i+1} - u_i \tag{4.2}$$

It is important to remark that not all the body must have the same stiffness. In some parts of the body (in this case near the contact area) the stiffness may vary from the global feature of the body. The stiffness near the contact area will be defined as contact stiffness.

Stiffness can vary depending on the geometry and material of the area under study. If a normal force is applied upon at body made of a homogeneous material (that is, same Young's modulus for all the geometry), the same reaction force will be found in all the cross sections of the geometry as we move vertically along the Y axis. But, if the geometry has different cross sections for different positions along Y, the same total reaction force is distributed in a smaller or larger area. Therefore, for smaller areas, the pressure and the deformation in that area will be larger, and thus the stiffness will be lower. For example, for the case of a rod of length l, cross section area A and Young's modulus E, the stiffness can be defined as in equation 4.3.

$$k = \frac{EA}{l} \tag{4.3}$$

The previous formula shows how the stiffness depends both on the material used and on the geometry of the body. In our case, the body will have a smaller cross section as we get near the contact area. Therefore, a higher deformation and a higher value of contact stiffness (locally speaking) are expected for a given load.

To conclude, the body will suffer a deformation due to the displacement and thus the contact area will become larger. In this problem, this can be summed up with the sketch shown in Fig. 4.3 .

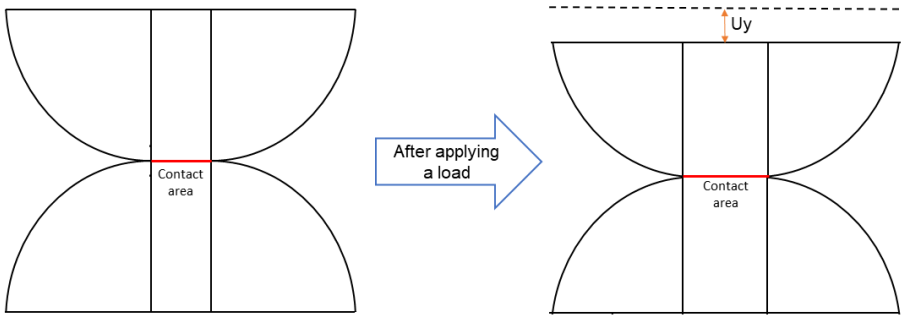

Fig. 4.3 Sketch of the deformation that the bodies will suffer upon application of the load/displacement in the top surface of the upper body

4.3 Numerical results using relative displacement

In order to understand how the contact stiffness varies with height, this parameter will be plotted for the three meshes previously defined (see Section 3.2). If the obtained results are similar for all three meshes, this will mean that it is mesh-independent.

The results will be obtained for the nodes along five main vertical axes on the flat punch, each axis with different horizontal position (that is, a different position in the X axis), as represented in Fig. 4.4. Only the vertical displacements (that is, Y-axis displacements) of the nodes along these vertical axes will be considered.

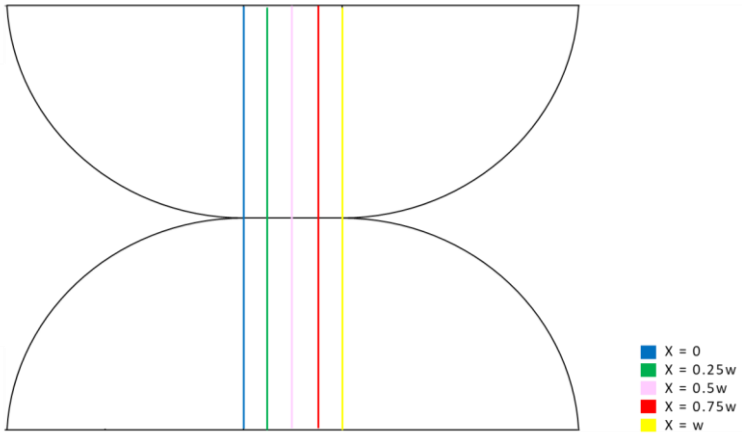

Fig. 4.4 Vertical axes of the body for which the displacement of their nodes along the Y axis will be considered

In order to have results that do not depend on the thickness of the body, the load per unit length (*P*) will be used. Therefore, the contact stiffness will be in [N/m/m] because it will be the contact stiffness per unit length. Particularly, as the applied displacement is in micrometres, the stiffness will be expressed as [N/μm/μm] in the results.

Notice that, as said in the previous chapter (see Section 3.4), *P* is a value obtained from the simulation and will vary depending on the mesh used. The meshes used in this problem are the same as the ones used in the mesh validation study but the displacement applied at the upper surface is smaller. As a consequence, the reaction force obtained will be smaller as well.

The reaction forces per unit length used in this problem are described in Table 4.2.

Table 4.2. Reaction force per unit length for each mesh in the normal contact problem, where a normal displacement is applied in the upper surface

Mesh	*P* (N/ μm)
1	0.0767
2	0.0762
3	0.0761

The results obtained with the three different meshes are shown in Fig. 4.5 and Fig. 4.6. In particular, the values of stiffness along the vertical axis can are presented. The plots were generated using MATLAB (see Appendix B.2).

Notice that the figures show only the plot for the vertical axes x = *w*, x = 0.25*w* and x = 0.5*w*, because the results for x = *w* and x = 0 are identical, as well as the results for x = 0.25w and x = 0.75w because of the symmetry of the body. For the average curve, the results of all 5 axes have been averaged. This average curve will give a general tendency of the stiffness in the flat punch.

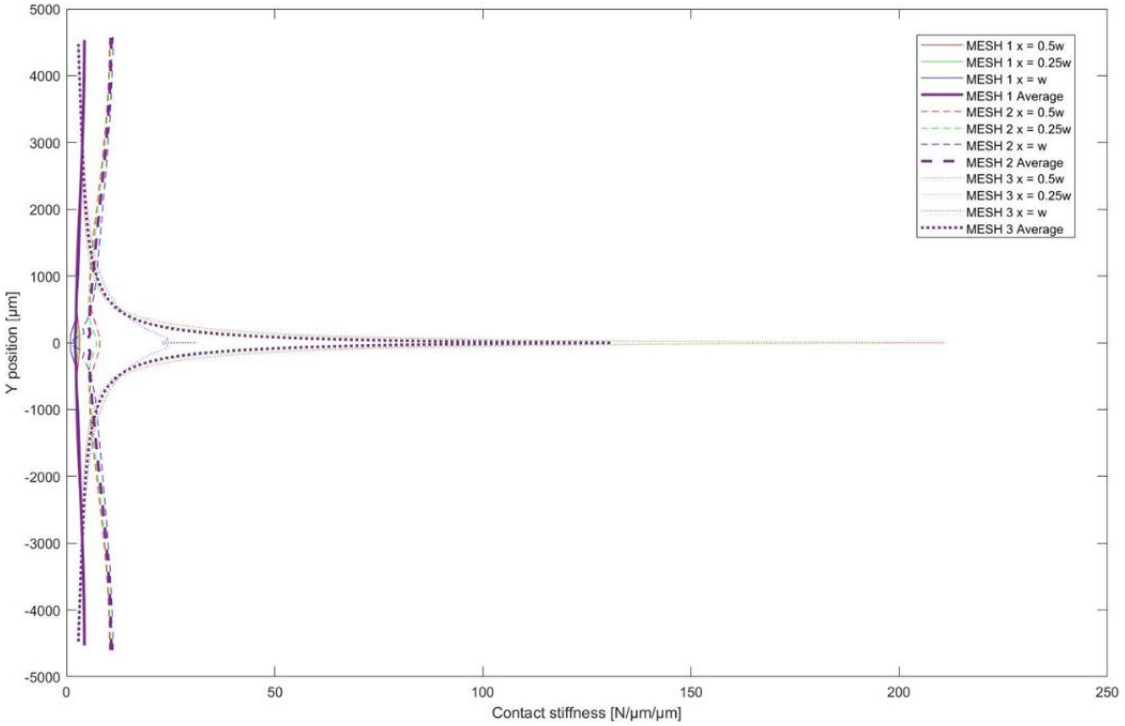

Fig. 4.5 Normal contact stiffness along the body for the flat punch when a normal displacement is applied in the upper surface

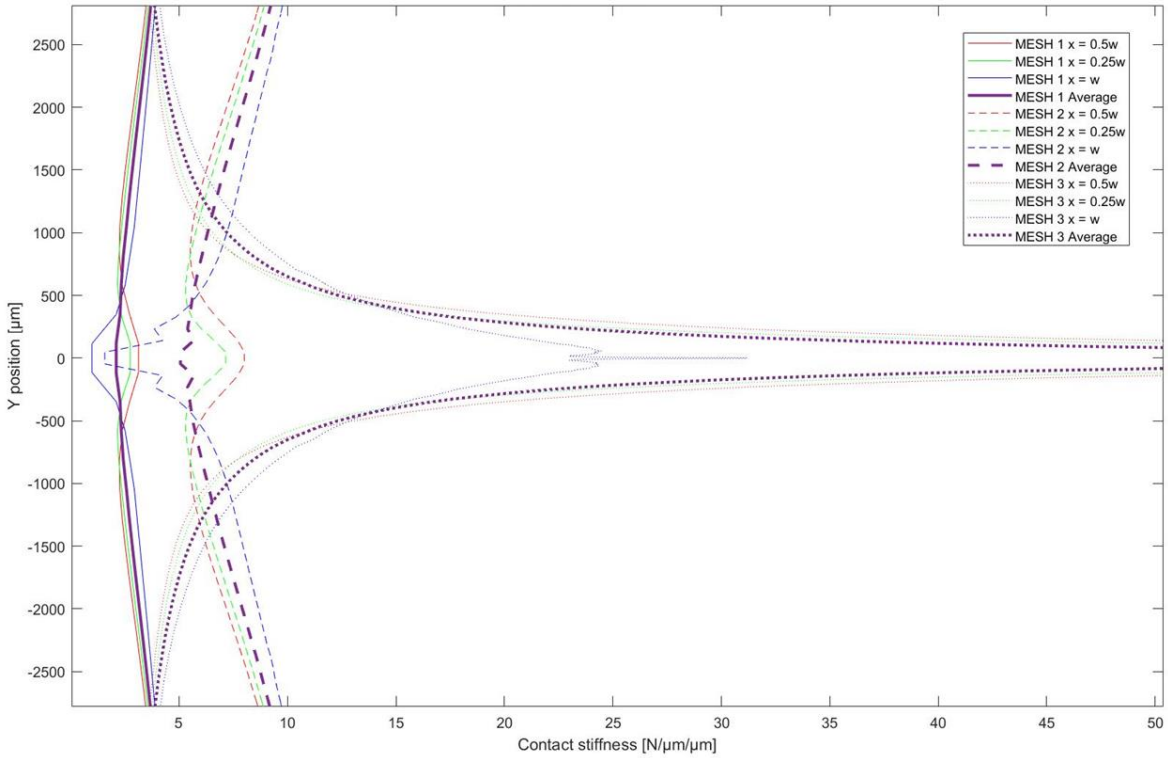

Fig. 4.6 Normal contact stiffness along the body for the flat punch when a normal displacement is applied in the upper surface (near the contact area)

As can be seen in the previous plots, for each of the three meshes, the results for various axes are similar far from the contact surface but, as we get closer to the contact area, they are more differences between them because near the contact area the number of elements and the size change a lot among the three meshes. Therefore, the results are not mesh-independent and they are not robust enough.

As the contact stiffness is related to the relative displacement of the nodes, and the position of the nodes depends on the mesh defined for that geometry, the results obtained are coherent because mesh 1 is the mesh that has bigger elements near the contact area and mesh 3 the one that has smaller elements. Therefore, the relative displacement of the nodes for the first mesh will be higher than for the third mesh and, for the same reason, the contact stiffness values will be lower for the first mesh, and they will increase as the elements in the contact surface becomes smaller.

Consequently, mesh 1 and 2 have a more realistic trend than mesh 3 because it was expected to obtain a smaller value of stiffness near the contact and, in the last case, it appears to be really high due to the small relative displacements.

Therefore, it is essential to find another definition for contact stiffness that does not depend on the mesh used to obtain robust solutions.

4.4 Numerical results using strain

Another way of defining contact stiffness is by the elastic strain, that is, by measuring the local deformation, which can be related to the normal relative displacement as follows:

$$\varepsilon_N = \frac{u_{rel\,N}}{l} \tag{4.4}$$

where ε_N is the normal elastic strain and l the distance between two consecutive nodes.

This way, the strain does not depend on the distance between two nodes (l), and the results are expected to be mesh-independent because they will not vary the position of the nodes defined by the used mesh. Notice that, in this case, the units for the contact stiffness per unit length using a load per unit length will be [N/μm/μm^2]. In this case, the normal contact stiffness per unit of length k_N^* for a normal force F_N can be written as follows.

$$k_N^* = \frac{k_N}{l} = \frac{F_N}{\varepsilon_N} \tag{4.5}$$

Considering the same vertical axes, meshes and reaction forces as in Section 4.3, the obtained results are shown in Fig. 4.7 and Fig. 4.8, as plotted with MATLAB (see Appendix B.3): the normal contact stiffness per unit length per unit length of the body calculated using strain is shown in Fig. 4.7 and, with more detail, in a zoom in centred in the contact area in Fig. 4.8.

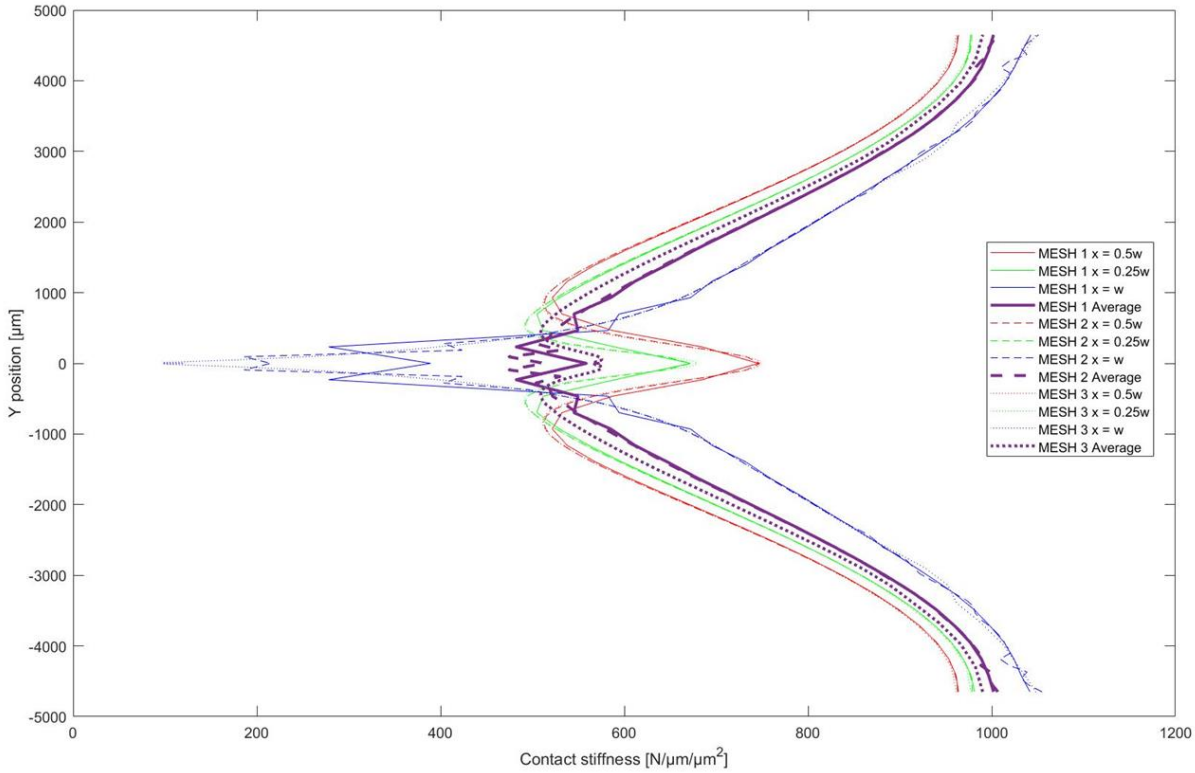

Fig. 4.7 Normal contact stiffness (calculated using strain) along the body for the flat punch when a normal displacement is applied in the upper surface

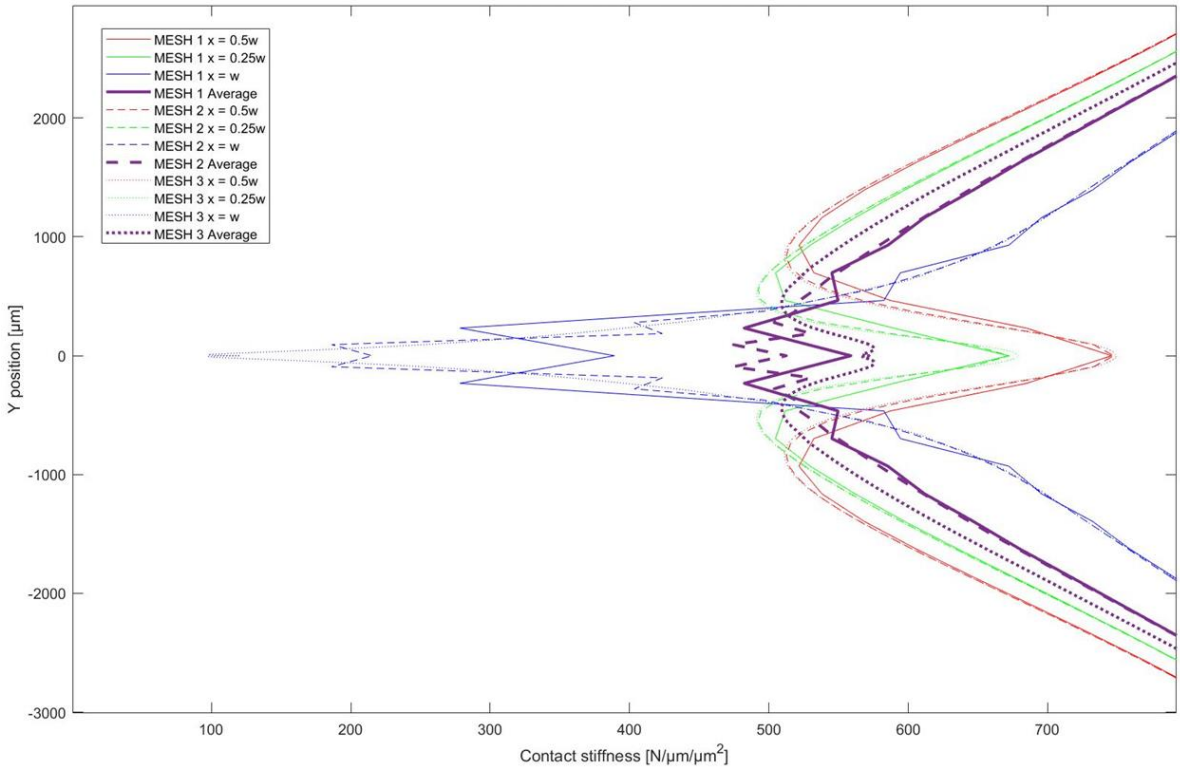

Fig. 4.8 Normal contact stiffness (calculated using strain) along the body for the flat punch when a normal displacement is applied in the upper surface (near the contact area)

As can be seen in the previous figures, the values of contact stiffness obtained are more similar between them for all meshes, even in the contact area. Thus, we can conclude that they are mesh-independent and, for that reason, robust results.

The general tendency, as can be seen in the average value curve, is to have smaller contact stiffness as we get closer to the contact area. This means that the body is more flexible in the contact area as it was expected because the cross section has a smaller area and consequently the stiffness becomes smaller as well (see Section 4.2).

These graphs give an idea of how contact stiffness evolves along the body, but the units are not the suitable ones, so it does not give the numerical value of this parameter. When relative displacements are used to obtain the contact stiffness (k), the correct units are obtained [N/m]. The contrary occurs when using elastic strain to obtain the contact stiffness (k^*), because the value obtained is the stiffness per unit length [N/m/m].

CHAPTER 5: Tangential contact problem

In this chapter, the contact stiffness will be studied when a tangential and a normal displacement are applied simultaneously among the body, and there is also a friction coefficient between the contact surfaces.

5.1 Contact model and boundary conditions

The contact model is the same as in the normal contact problem (see Section 4.1) but boundary conditions change. In this problem, friction is introduced and displacement in the horizontal direction is applied in the upper surface. Therefore, there are two displacements applied, one tangential (*Ux*) and one normal (*Uy*) to the upper surface and, in consequence, the reaction force can be decomposed into the tangential force (*Px*) and the normal force (*Py*). This can be seen more clearly in Fig. 5.1.

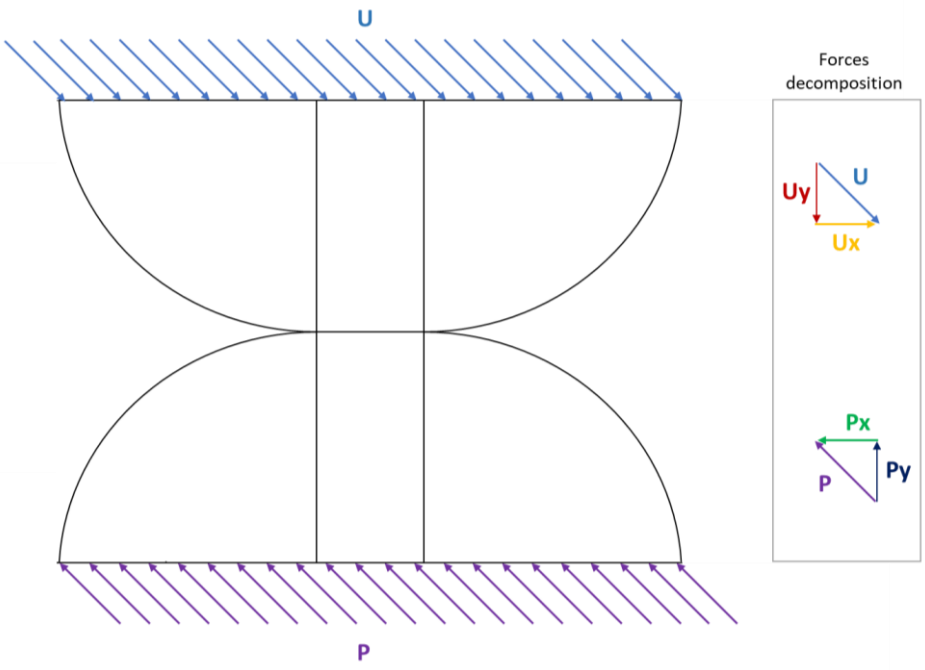

Fig. 5.1 Sketch of the normal (*Uy*) and tangential displacement (*Ux*) and the reaction force (*P*) in the top surface of the upper body and the bottom surface of the lower body, respectively

Notice that Fig. 5.1 is a 2D sketch of the cross section, but the displacement and the reaction force are applied along all the thickness of the body (third dimension, normal to the cross section).

The parameters used for this contact model are listed in Table 5.1.

Table 5.1. Values of the parameters used in the tangential contact problem, when a normal and a tangential displacement are applied in the upper surface and there is friction in the contact surface

Parameter	Value	Units
Normal displacement (*Uy*)	-1	μm
Tangential displacement (*Ux*)	-1	μm
Friction coefficient (*μ*)	0.5	-
Radius of curvature (*R*)	4650	μm
Width of the flat punch (*w*)	1550	μm
Thickness (*TH*)	7750	μm
Young's modulus (*E*)	205	GPa
Poisson ratio (*v*)	0.3	-

5.2 Mesh validation for the tangential problem

Before finding the results of the contact stiffness, as a tangential force and a friction coefficient are introduced in this chapter, it is necessary to check if the mesh selected as the most refined (see CHAPTER 3) is still accurate for this model.

The tangential force and the friction may modify the pressure distribution obtained with numerical results. Therefore, to study the variation the tangential force or the friction might produce to the results, a comparison between three cases has been performed with the same geometry as in the mesh validation (see Section 3.1), to validate the most refined mesh for this problem:

- CASE 1: Applying a normal displacement (*Uy* = -25 μm) on the upper surface without friction between the contact surfaces.

- CASE 2: Applying a normal displacement (*Uy* = -25 μm) on the upper surface with friction between the contact surfaces (*μ* = 0.5).

- CASE 3: Applying a normal (*Uy* = -25 μm) and a tangential displacement (*Ux* = 1 μm) on the upper surface with friction between the contact surfaces (*μ* = 0.5).

The comparison of the analytical results and the numerical results obtained for the pressure distribution can be seen in Fig. 5.2

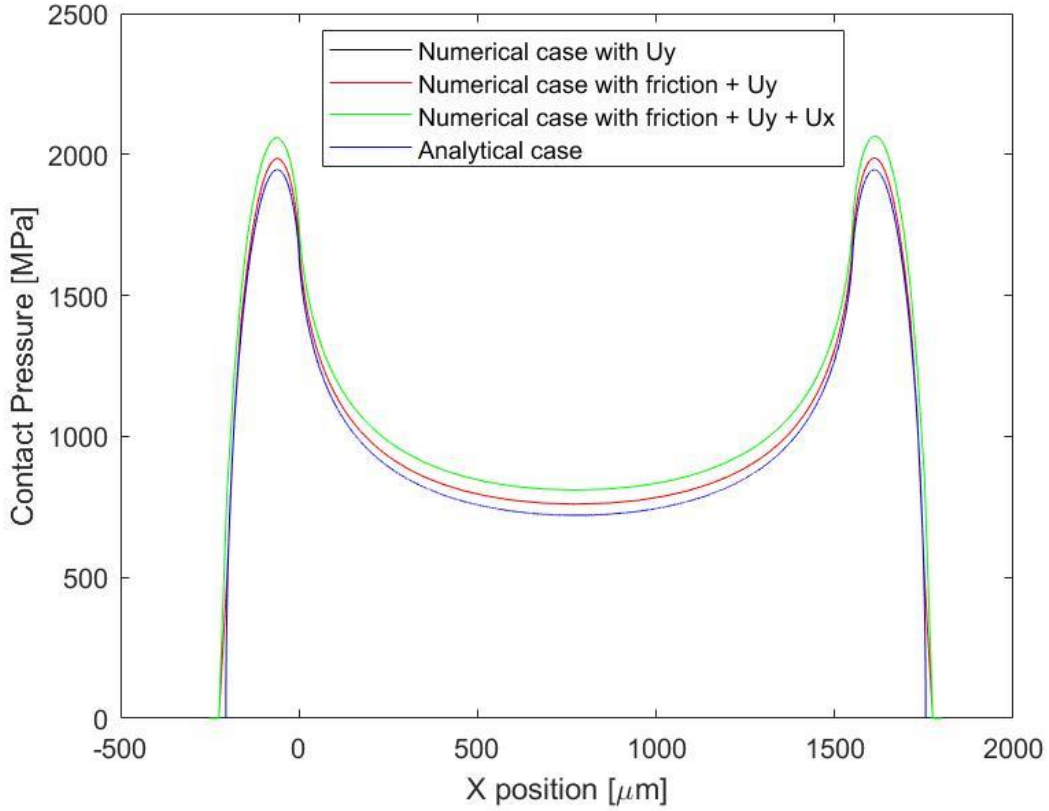

Fig. 5.2 Normal pressure distribution of the analytical and numerical case applying a normal displacement, a normal displacement and friction and a normal displacement, a tangential displacement and friction

As can be seen, the results for the cases with normal displacement, with and without friction, have the same results. Then, it can be concluded than the application friction between the surfaces does not affect the normal pressure distribution in the contact area. Contrarily, there is a difference between Case 1 and Case 2 with respect to Case 3, due to the tangential displacement.

The errors between analytical and numerical results for Case 3 are stated in Table 5.2.

Table 5.2. Absolute and relative errors of the pressure distribution for the numerical results of Case 3 with friction with respect to the analytical results

X Position (μm)	Absolute error (MPa)	Relative error (%)
-62	114.0	5.86
0	106.0	6.45
500	89.0	11.75
775	89.7	12.45
1000	89.7	12.05
1550	111.0	6.76
1612	119.5	6.14

The relative errors when a tangential displacement is introduced increase from 2-6% (see Table 3.6), where only a normal displacement was applied, to 5-13%.

The variation of the numerical results between Case 1 and Case 3 (that is, when a tangential displacement is introduced) is stated by K.L. Johnson [11]. The elastic displacements on the surface are deduced by the summation of the displacements due to concentrated forces. If $p(x)$ is the normal pressure distribution and $q(x)$ the tangential pressure distribution, the normal and tangential displacements at point C can be stated in equations 5.1 and 5.2.

$$u_x = -\frac{(1-2v)(1+v)}{2E}\left\{\int_{-b}^{x} p(s)ds - \int_{x}^{a} p(s)ds\right\} - \frac{2(1-v^2)}{\pi E}\int_{-b}^{a} q(s)ln|x-s|ds + C_1 \quad \textbf{(5.1)}$$

$$u_y = \frac{(1-2v)(1+v)}{2E}\left\{\int_{-b}^{x} q(s)ds - \int_{x}^{a} q(s)ds\right\} - \frac{2(1-v^2)}{\pi E}\int_{-b}^{a} p(s)ln|x-s|ds + C_2 \quad \textbf{(5.2)}$$

where u_x is the tangential displacement, u_y is the normal displacement, and the rest of the parameters are in the sketch of Fig 5.3 .

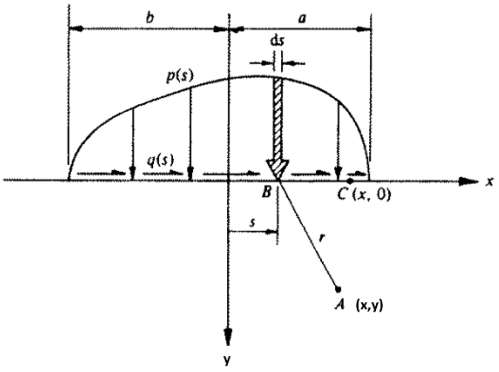

Fig 5.3 Parameters of a figure used to find the tangential and normal elastic displacements in point C [11]

As can be seen, both normal and tangential displacements are affected by the normal and tangential pressure. Consequently, the normal pressure values will change if a tangential displacement is applied and, therefore, the reaction force will vary as well as can be seen in Table 5.3

Table 5.3. Difference between reaction forces at the bottom when friction or a normal and a tangential displacement are applied

	Reaction force at the bottom (N)
CASE 1 (*Uy*)	15720
CASE 2 (*Uy* + *μ*)	15721
CASE 3 (*Uy* + *Ux* + *μ*)	16813

It is also useful to study the shear distribution for the numerical results and comparing it to the analytical results in order to see if the mesh is refined enough for obtaining the tangential contact stiffness, not only the normal contact stiffness. In order to do so, a 2D model by Shtayerman has been used as reference [10]. The model states that, for a flat punch with rounded edges on top of a semi-infinite plane, it can be shown that the shear stress $q(x)$ is equal to the difference between the actual pressure distribution $p(x)$ and the pressure distribution for a smaller contact area $p*(x)$ multiplied by the coefficient friction μ. The shear stress can be also written as a superimposition of two functions, as it is stated in the following equation.

$$q(x) = \mu p(x) - q*(x) \;=\; \mu[p(x) - p*(x)] \tag{5.3}$$

The $q*(x)$ expression depends only on the ratio a/c where c is the half width of the central stick area after, which is unknown. The a/c ratio can be found with the next equation.

$$\frac{2PR}{a^2E^*}\left(1 - \frac{Q}{\mu P}\right) = \frac{\pi - 2\theta_0}{2\sin^2\theta_0} - \cot\theta_0 \tag{5.4}$$

where Q is the applied tangential force per unit length and $\sin\theta_0 = a/b$.

The equation 5.4 is solved with numerical methods to find θ_0 and therefore a/c.

Then, $q*(\varphi)$ is provided by the next equation.

$$q*(\varphi) = \frac{\mu P - Q}{c}\, f(\varphi_0, \varphi) \tag{5.5}$$

where $\sin\theta = x/c$ and $f(\theta_0, \theta)$ is defined as:

$$f(\theta_0,\theta) = -\frac{2/\pi}{\pi - 2\theta_0 - \sin 2\theta_0}\left\{(\pi - 2\theta_0)\cos\theta + ln\left[\left|\frac{\sin(\theta+\theta_0)}{\sin(\theta-\theta_0)}\right|^{\sin\theta}\left|\tan\frac{\theta+\theta_0}{2}\tan\frac{\theta-\theta_0}{2}\right|^{\sin\theta_0}\right]\right\} \tag{5.6}$$

Finally, taking the parameters P, R, w, E, v, Q and μ as known, the shear stress distribution is defined applying the previous formulas in a MATLAB code (see Appendix B.4) as Fig. 5.4 shows.

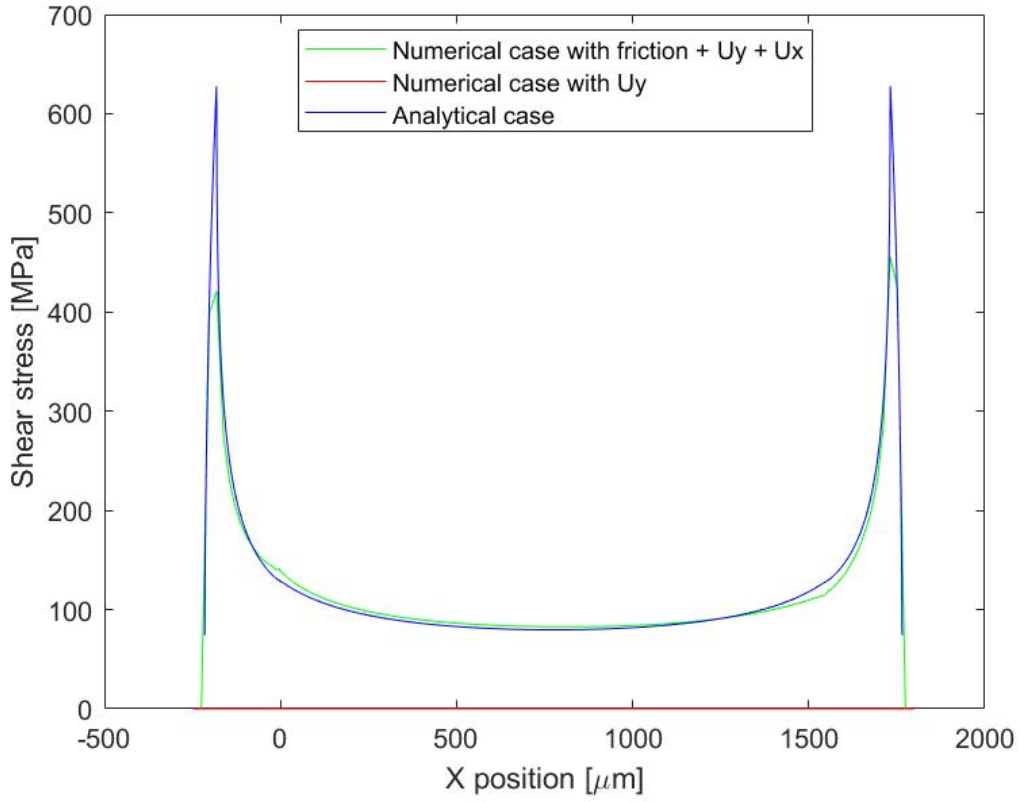

Fig. 5.4 Shear distribution of the analytical and numerical case applying a normal displacement, a normal displacement and friction and a normal displacement, a tangential displacement and friction

As can be seen in the previous plot, there is no shear stress for the case where there is not a tangential displacement, as it was to expect. Furthermore, the numerical results for the case with friction and a normal and tangential displacement are very close to the analytical results but there are some notable differences at the edges (x = -182 µm and x = 1732 µm), as can be seen in Table 5.4. Then, it can be concluded that this mesh is refined enough to be used in a problem, where not only a normal displacement but a tangential displacement is also applied.

Table 5.4. Absolute and relative errors of the shear distribution for the numerical results with friction and a normal and tangential displacement with respect to the analytical results

X Position (µm)	Absolute error (MPa)	Relative error (%)
-182	206.6	32.91
0	10.7	8.33
500	3.5	4.17
775	3.1	3.83
1000	2.2	2.69
1550	8.4	7.11
1732	171.6	27.34

5.3 Tangential contact stiffness definition

In this case, not only normal contact stiffness (k_N), but also tangential contact stiffness (k_{tan}) is considered, using the tangential force (F_{tan}) and tangential displacement ($u_{rel\,tan}$). Then, the tangential contact stiffness can be expressed as follows:

$$k_{tan} = \frac{F_{tan}}{u_{rel\,tan}} \tag{5.7}$$

As seen in the previous problem (see Section 4.3), the numerical values obtained using the previous definition will not be mesh-independent. For that reason, in this problem, only the results obtained with the elastic strain will be considered. The tangential contact stiffness per unit length can be defined as:

$$k^*_{tan} = \frac{F_{tan}}{\varepsilon_{tan}} \tag{5.8}$$

where k^*_{tan} is the tangential contact stiffness per unit length and ε_{tan} is the tangential elastic strain.

5.4 Numerical results using strain

The results have been obtained directly using elastic strain. Besides, the most refined mesh (mesh 3) will be used because, as seen in Section 4.4, the results obtained with elastic strain are mesh-independent.

In Table 5.5, the values of the obtained reaction forces are listed.

Table 5.5. Reaction force per unit length in the X and Y directions for mesh 3 in the tangential contact problem

Mesh	*Py* (N/ µm)	*Px* (N/ µm)
3	0.0812	0.0809

The results for the normal contact stiffness are shown in Fig. 5.5 and Fig. 5.6 .

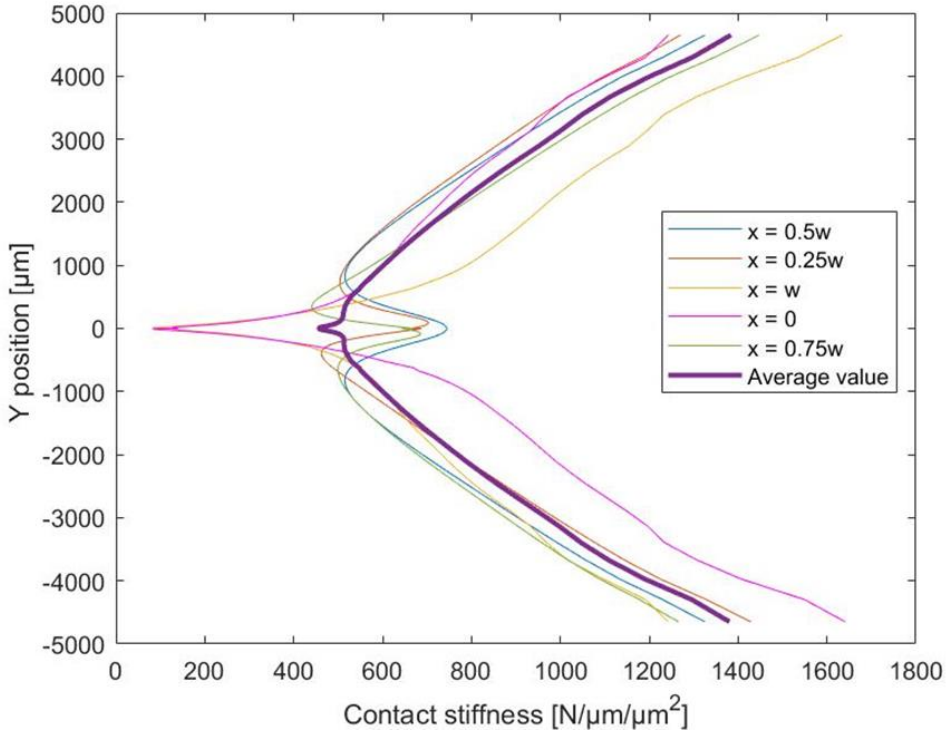

Fig. 5.5 Normal contact stiffness (calculated using strain) along the body for the flat punch, when a normal and a tangential displacement are applied in the upper surface and there is friction in the contact surface

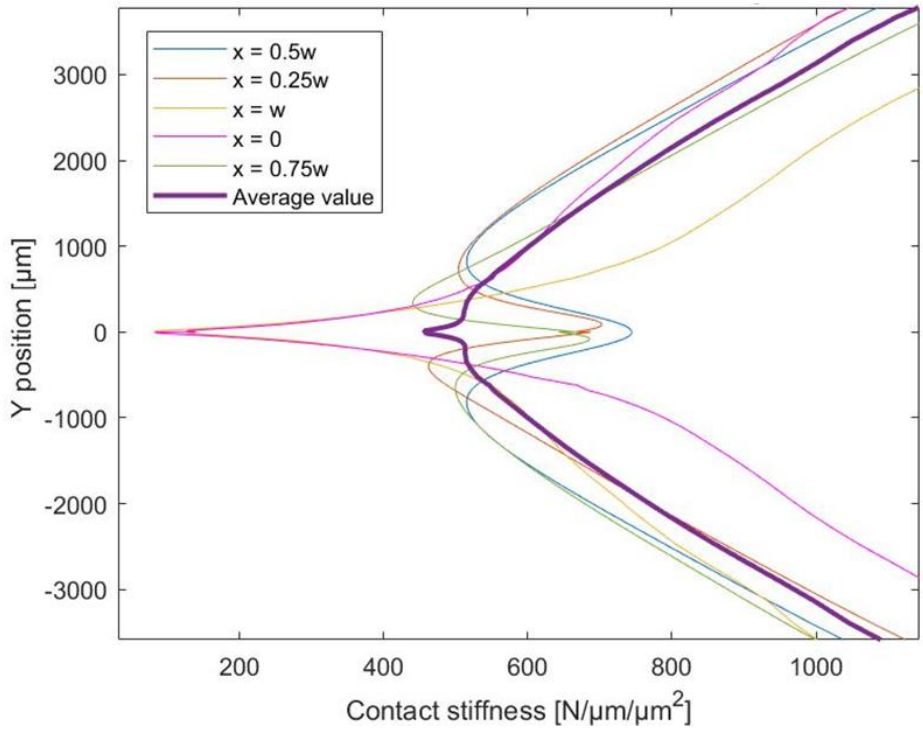

Fig. 5.6 Normal contact stiffness (calculated using strain) along the body for the flat punch, when a normal and a tangential displacement are applied in the upper surface and there is friction in the contact surface (near the contact area)

In the previous plots, the normal contact stiffness in the studied case was plotted along the five vertical axes and the average value of all of them. As can be seen, the average value is symmetric with respect to the contact area (Y axis). Nevertheless, if we look into each of the axes individually, the only symmetric results with respect to the Y axis are the ones obtained with the middle axis (x = *w*/2). It is important to remark that the other axes are located in symmetric X-positions (x = 0 with x = *w* and x = 0.25*w* with x = 0.75*w*) and the results obtained will be symmetric with respect to the Y axis for each couple of axes, because the contact stiffness of the upper body is the opposite of the contact stiffness of the lower axis for the same position and vice versa due to the friction force variation.

The friction force variation can be seen more clearly in Fig. 5.7, which shows a sketch of a random body where a tangential displacement (*Ux*) is applied. The body is on top of another body with friction between them. The blue axes of the upper and lower body have opposite positions with respect to the middle vertical axis, but the same friction force because both are in contact with the air and not with a solid surface, so the friction coefficient will decrease. The same phenomenon occurs for the green axes, which are in contact with a solid surface and not with air, and therefore the friction coefficient will increase. That is the reason why the results along the axes x = 0 and x = *w*, and x = 0.25*w* and x = 0.75*w*, are symmetric between them with respect to the vertical middle axis.

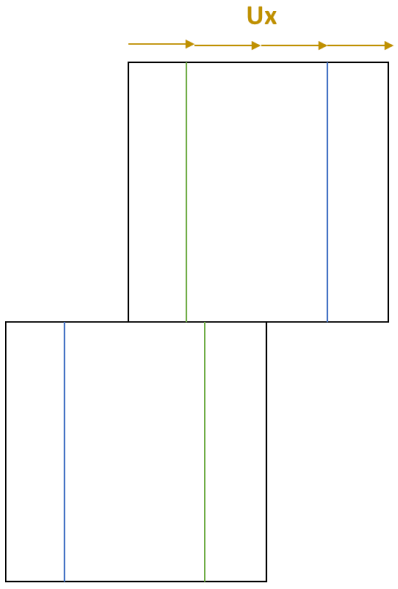

Fig. 5.7 Sketch of axes of two random bodies with same the friction force for opposite positions symmetric to the middle axis

In Fig. 5.8 and Fig. 5.9, the tangential contact stiffness is presented obtained from the tangential elastic strain.

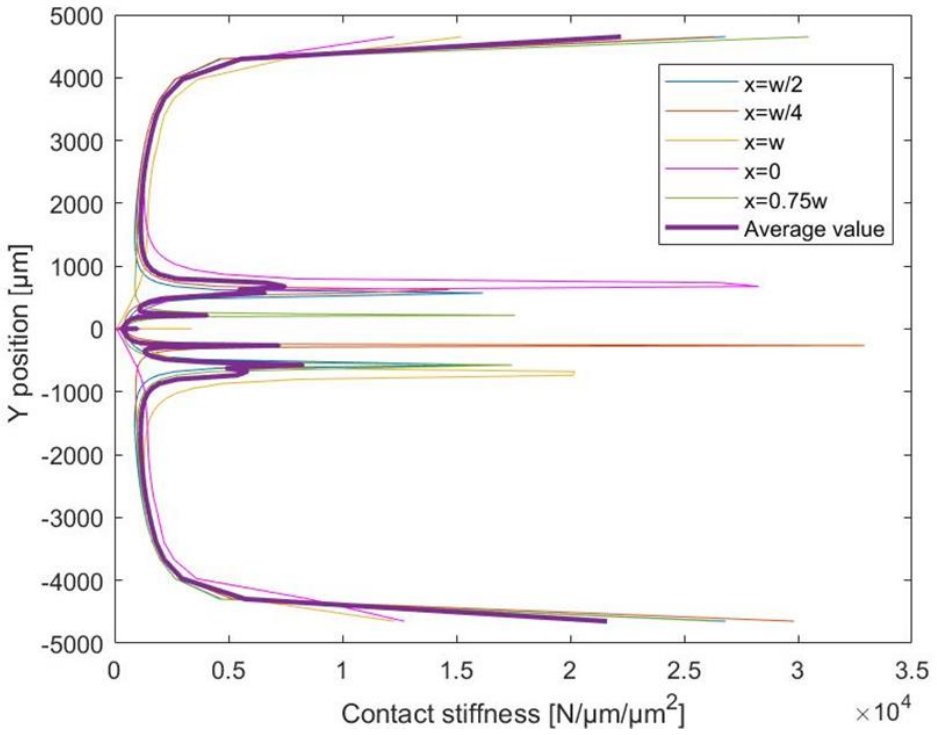

Fig. 5.8 Tangential contact stiffness (calculated using strain) along the body for the flat punch, when a normal and a tangential displacement are applied in the upper surface and there is friction in the contact surface

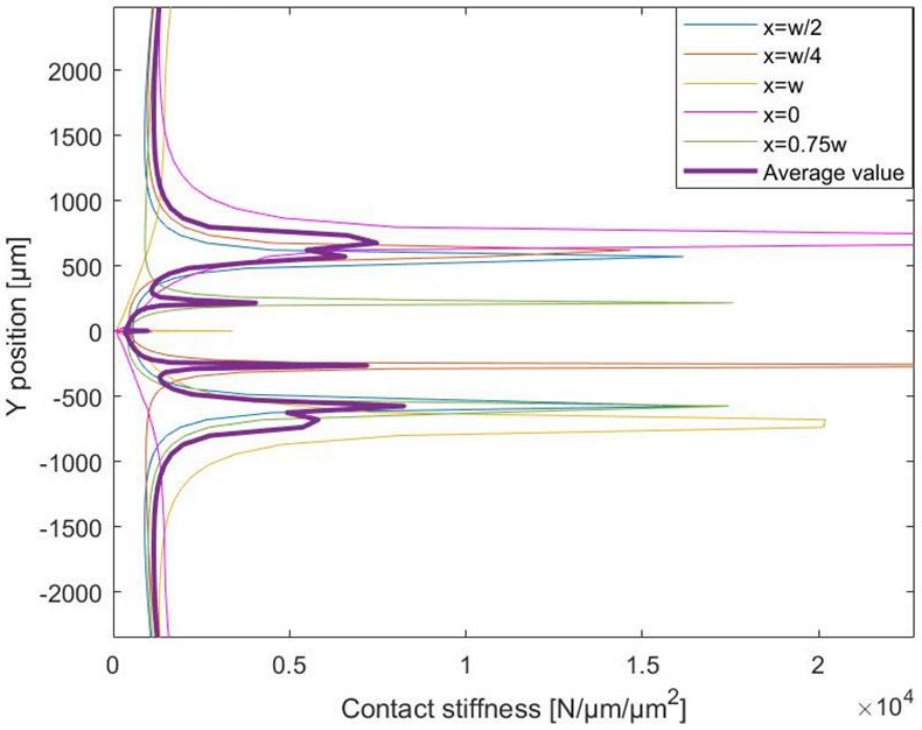

Fig. 5.9 Tangential contact stiffness (calculated using strain) along the body for the flat punch, when a normal and a tangential displacement are applied in the upper surface and there is friction in the contact surface (near the contact area)

Unfortunately, these plots about the tangential contact stiffness do not give information about the pattern that the contact stiffness follows. From a general point of view, the stiffness is larger as we move far from the contact area but there are also some stiffness peaks. Near the contact surface, the irregular shape may be due to mesh used because, as seen in Section 5.2, there is some variation of the analytical and numerical results of shear distribution in the contact surface at the edges that may cause some errors in the numerical results obtained. In conclusion, these results will also be discarded.

CHAPTER 6. Conclusions and future work

6.1 Conclusions

This work investigates the possibility of defining the contact stiffness of a flat punch friction contact. When two flat punches with rounded edges are pressed together, a variable local stiffness pattern of contact stiffness can be appreciated and the dependency of the results with the quality of the mesh is studied. The obtained results lead to the following conclusions:

- From the mesh validation, analytical results for the pressure distribution in the contact surface were obtained. The distribution is symmetric with respect to the vertical middle axis because the defined contact model is also symmetric. Moreover, the pressure is significantly higher in the edges of the contact surface compared to the central region because the body suffers a larger deformation and therefore larger stresses in that area (the force is concentrated in that region).

- From the mesh validation, numerical results for the pressure distribution in the contact surface were obtained, with three meshes with different level of refinement (mesh 1 (coarse), 2 (medium) and 3 (fine)). The numerical results have a relative error with respect to the analytical results of 8-120% for mesh 1, 9-54% for mesh 2 and 2-6% for mesh 3. The relative error can be due to the mesh configuration because the mesh can be in some cases too coarse with respect to the level of detail that is required by the contact geometry. The higher relative errors are found in the peaks of the pressure distribution (that is, on the edges of the contact area). The fact that mesh 3 produced a smaller relative error is in agreement with expectation since it has the highest number of elements along the contact punch. Consequently, mesh 3 is chosen to perform the study of the contact stiffness and the results obtained with mesh 3 will be considered as precise and robust enough.

- From numerical results on the normal contact stiffness calculated by using nodal displacements, we can conclude that the contact stiffness distribution along the vertical axis of the body is mesh-dependent and consequently, not robust. The results obtained with the three meshes are more similar far from the contact surface and have significant differences near the contact surface because near the contact area the number of elements and the size change a lot among the three meshes. Furthermore, mesh 1 and 2 have a more realistic trend than mesh 3 because it was expected to obtain a smaller value of stiffness near the contact due to higher deformations and, with mesh 3, contact stiffness appears to be really high due to the small relative displacements because of the extremely refined mesh. It can be concluded that mesh 3 is the most refined but gives really high values of contact stiffness near the contact surface, that are not coherent with reality.

- From numerical results on the normal contact stiffness obtained by using strain, we can conclude that the contact stiffness per unit length (that is, using elastic strain) is mesh-independent and consequently, robust. The general tendency of the obtained values is as expected: a smaller contact stiffness per unit length near the contact area due to higher deformations. However, the contact stiffness per unit length [N/m/m] does not give the numerical value of an actual contact stiffness [N/m] (quantitative values) but only the tendency that it follows (qualitative values).

- From the mesh validation for the tangential contact problem, we can conclude that if a tangential displacement is introduced, the numerical results for the normal pressure distribution change slightly: For the most refined mesh, these results have an error of 5-13% with respect to the analytical results (recall that, without tangential displacements, the error was 2-6%). The variation of the numerical results in the presence of a tangential displacement with respect to the analytical results of the normal pressure distribution is due to the variation of the normal displacements in the presence of the friction forces, as stated in [11]. It can also be concluded that the presence of friction does not affect the pressure distribution results.

- From the mesh validation for the tangential contact problem, we can conclude that the mesh selected as most refined (mesh 3) in tangential contact problem gives relative errors of the numerical results with respect to the analytical ones for the shear stress of 2 to 35%. This can produce some errors when estimating the tangential contact stiffness due to the mesh selected.

- The general tendency of the normal contact stiffness per unit length obtained numerically is as expected: smaller values near the contact area. Due to the friction force variation, only the middle vertical axis has symmetric results with respect to the contact area. The results obtained for the tangential contact stiffness have been discarded because they do not give information about the pattern that the contact stiffness follows, probably because the mesh used is not refined enough for a tangential contact problem.

6.2 Future work

Finally, the different future implementations and improvements of this project are proposed and listed below.

- An experimental validation of the results obtained was initially going to be performed in the laboratory to check the results obtained with the physical phenomenon. This part could not be performed because of restrictions due to the global pandemic.

- Furthermore, it is important to delimitate the contact area to characterize the contact behaviour correctly. Normally, in engineering, the contact surface is very easy to define from a practical point of view because the joint is very small in comparison with the large structure where it is used.

  It was seen that the results from Section 4.3 were mesh-dependent because the relative displacements depended on the mesh selected. Therefore, if the contact area is well delimitated, the nodes that will delimitate the contact area will be fixed and therefore the relative displacement between them will not change with the mesh. An example would be applying different displacements to the same model and studying the reaction force obtained. Then, the contact stiffness can be defined as the relation between the displacements and the reaction force, as can be seen in Fig. 6.1 with equation 6.1.

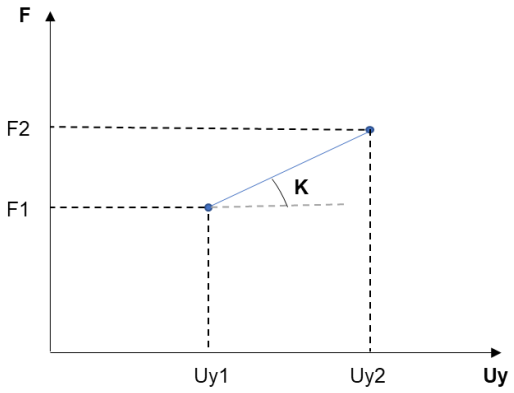

Fig. 6.1 Contact stiffness definition as the relation between the displacements and the reaction forces when two simulations are performed with different displacements applied

$$k = \frac{F_2 - F_1}{Uy_2 - Uy_1} \quad \textbf{(6.1)}$$

- Another proposed method to find the patterns of the contact stiffness and its numerical values with mesh-independent results is loading. That is, varying the height position where the displacement is applied and calculating the stiffness only between two nodes: the first one where the displacement is applied and the other one where the body ends. If the contact area is well defined, the stiffness can be easily found by using equation 4.1.

Bibliography

[1] Lambda Technologies Group. Fretting. *Fretting Damage Location on Dovetail Joint*. [CorssRef]

[2] G. Battiato, C. M. Firrone, "*Reduced order modelling of large contact interfaces to calculate the non-linear response of frictionally damped structures*" in Procedia Structural Integrity. 24, 837-851 (2019). [CrossRef]

[3] D. L. Heiserman. Fundamentals of Aircraft Gas Turbine engines. *Turbine construction*. [CrossRef]

[4] Ansys. ANSYS Mechanical APDL Command Reference (2010). Available online: https://www.mm.bme.hu/~gyebro/files/ans_help_v182/ans_cmd/Hlp_C_CmdTOC.html

[5] E. Correa Allepuz, "*Optimización del difusor con álabes del compresor centrífugo de una planta de desalación mediante CFD*" Universidad de Sevilla. Appendix 1. 143-147 (2005)

[6] S. Sezen, "*An evaluation of ANSYS contact elements*" Louisiana State University Master's Theses. 60 (2005). [CrossRef]

[7] C. M. Firrone, "*Guida introduttiva all'utilizzo degli elementi di contatto di Ansys.*" Dipartimento di Meccanica, Politecnico di Torino (2009).

[8] E. Wang, "*Penalty vs. Lagrange. ANSYS contact.*" CADFEM GmbH. (2004). Available online: https://slideplayer.com/slide/6816372/

[9] R. Anstee, "*The Newton-Raphson Method*" Mathematics Department, University of British Columbia. (2006). [CrossRef]

[10] I. Y. Shtayerman, "*Contact problem of the theory of elasticity.*" Moscow-Leningrad (1949) 102-185. [CrossRef]

[11] K. L. Johnson, "*Contact mechanics.*" Cambridge University Press. 18-21 (1985).

APPENDIX A. Parametric design

In this appendix, an example of the parametric design used for defining a finite element is described. The parametric design that sets up the model is written in a .txt file and imported to Ansys in order to be solved. Particularly, the case the .txt file used in the normal contact problem with refined mesh is presented.

```
FINISH
/CLEAR,START
/PREP7

! DEFINE ELEMENTS !
ET,1,MESH200                ! Not solved element
KEYOPT,1,1,6                ! 3-D Quadrilateral 4 nodes
ET,2,SOLID185               ! 3-D 8-Node Structural Solid (+ mid side nodes 186) !

! DEFINE MATERIAL PROPERTIES!
MP,EX,1,0.205               ! Young Modulus  [N/micron^2]
MP,PRXY,1,0.3               ! Poisson Coefficient
MP,DENS,1,1                 ! Density [kg/(m^3) ]

! DEFINE GEOMETRY !
w = 1550                    ! Width flat punch  [micron]
r = 3*w                     ! Radius rounded edge (micron)
th = 5*w                    ! Thickness (micron)
EL_cw = 30                  !  Element division of the lines of the contact width (contact width)
EL_ce = 25                  ! Element division of the lines of the round edge close to the flat
                            contact edge (potential contact)
EL_m = 60                   ! Element division of the lines close to the potential contact area
                            (round edge)
EL_f = 12                   ! Element division of the lines of the further part (further part)
EL_v = 60                   ! Element division of the vertical lines (vertical lines)

! DEFINE KEY POINTS!
K,1,0,0, 0                  ! K1
K,2,w,0,0                   ! K2
K,3,r+w,r,0                 ! K3
K,4,w,r,0                   ! K4
K,5,-r,r,0                  ! K5
K,6,0,r,0                   ! K6

! DEFINE LINES !
L,1,2                       ! L1
L,2,4                       ! L2
L,4,6                       ! L3
L,6,1                       ! L4

! DEFINE AEREAS !
AL,1,2,3,4                  ! A1
larc,2,3,4,r                ! L5
L,3,4                       ! L6
AL,5,6,2                    ! A2
larc,1,5,6,r                ! L7
L,5,6                       ! L8
AL,7,8,4                    ! A3

! DIVIDE AREAS !
K,7,r+w,0,0                 ! K7
L,4,7                       ! L9
```

```
ASBL,2,9                    ! Extract line 9 from area 2
K,9,-r,0,0                  !K9
L,6,9                       ! L10 (new L5)
ASBL,3,5                    ! Extract line 10 (new line 5) from area 3
k,10,w+100,0,0              ! K10
L,4,10                      ! L11 (new L5)
ASBL,4,5                    ! Extract line 11 (new line 5) from area 4
k,11,-100,0,0               ! K11
L,6,11                      ! L12 (new L5)
ASBL,2,5                    ! Extract line 11 (new line 5) from area 2

! DEFINE MESH 2D !

allsel,all
LESIZE,7,,,EL_ce,10, , , ,1     ! Divide lines in divisions of EL_ce with a ratio of 10
LESIZE,10,,,EL_ce,10, , , ,1
LESIZE,16,,,EL_m,0.25           ! Divide lines in divisions of EL_m with a ratio of 0.25
LESIZE,18,,,EL_m,0.25
LESIZE,6,,,EL_f                 ! Divide lines in divisions of EL_f
LESIZE,8,,,EL_f
LESIZE,13,,,EL_f
LESIZE,11,,,EL_f
LESIZE,12,,,EL_f
LESIZE,14,,,EL_f

FLST,2,2,4,ORDE,2           ! Division of the central lines of the flat punch in two
FITEM,2,1
FITEM,2,3
LDIV,P51X, , ,2,0
LSTR,12,11                  ! L19
ASBL,1,19                   ! Extract line 19 from area 1

LESIZE,19, , ,EL_v,0.01, , , ,1  ! Division of the vertical lines
LESIZE,2, , ,EL_v,100, , , ,1
LESIZE,4, , ,EL_v,0.01, , , ,1
LESIZE,15, , ,EL_v,0.01, , , ,1
LESIZE,17, , ,EL_v,0.01, , , ,1

LESIZE,1, , ,EL_cw,40, , , ,1    ! Division of half flat punch central area with EL_cw divisions
LESIZE,3, , ,EL_cw,40, , , ,1
LESIZE,5, , ,EL_cw,0.025, , , ,1
LESIZE,9, , ,EL_cw,0.025, , , ,1

! MESH AREA !
Type,1                      ! Select element type number
MSHAPE,0,2D                 ! Shape and dimension
MSHKEY,1                    ! Mapped meshing
AMESH,9                     ! Mesh central area (A9)
AMESH,2                     ! Mesh central area (A2)
MSHKEY,0                    ! Free meshing
AMESH,3,4,1                 ! Mesh the rest (A3, A4)
AMESH,5,8,1                 ! Mesh the rest (A5,A6,A7,A8)

! DEFINE MESH 3D !

MAT,1                       ! Select material
TYPE,2                      ! Select element type number
ESIZE,,12                   ! Divisions of the boundary lines (bricks on thickness)
VOFFST,6,-th                ! Generates volume of area 6 with thickness th
VOFFST,8,-th                ! Generates volume of area 8 with thickness th
```

```
VOFFST,4,-th                ! Generates volume of area 4 with thickness th
VOFFST,2,th                 ! Generates volume of area 2 with thickness th
VOFFST,3,th                 ! Generates volume of area 3 with thickness th
VOFFST,7,th                 ! Generates volume of area 7 with thickness th
VOFFST,5,th                 ! Generates volume of area 5 with thickness th
VOFFST,9,th                 ! Generates volume of area 9 with thickness th
nummrg,all                  ! Merge coincident or equivalently defined items
VSYMM,Y,all                 ! Generates volume by symmetry

! DEFINE NODES COMPONENTS !
ASEL,S, , ,11,24,13         ! Select area 11 & 24
ASEL,A, , ,36               ! Select area 36
ASEL,A, , ,41               ! Select area 41
nsla,s,1                    ! Select all nodes on the areas
CM,nodes_top,NODES          ! Create component

ASEL,S, , ,33,53,20         ! Select area 33 & 53
ASEL,A, , ,66               ! Select area 66
ASEL,A, , ,70               ! Select area 70
nsla,s,1                    ! Select all nodes on the areas
CM,nodes_bottom,NODES       !Create component

ASEL,S, , ,18,22,4          ! Select area 18 & 22
ASEL,A, , ,27               ! Select area 27
ASEL,A, , ,39               ! Select area 39
nsla,s,1                    ! Select all nodes on the areas
CM,nodes_contact_top,NODES      !Create component

ASEL,S, , ,47,51,4          ! Select area 47 & 51
ASEL,A, , ,56               ! Select area 56
ASEL,A, , ,69               ! Select area 69
nsla,s,1                    ! Select all nodes on the areas
CM,nodes_contact_bottom,NODES   ! Create component

NSEL,S,LOC,X,w/2            ! Select the nodes at the axis x=w/2
NSEL,R,LOC,Z,th/2
CM,nodes_major_axis,NODES   ! Create component

NSEL,S,LOC,X,w/4,403        ! Select the nodes at the axis x=w/4
NSEL,R,LOC,Z,th/2
CM,nodes_major_axis2,NODES      ! Create component

NSEL,S,LOC,X,w-1,w+1        ! Select the nodes at the axis x=w
NSEL,R,LOC,Z,th/2
CM,nodes_major_axis3,NODES      ! Create component

NSEL,S,LOC,X,-1,1               ! Select the nodes at the axis (x=0)
NSEL,R,LOC,Z,th/2
CM,nodes_major_axis4,NODES      ! Create component

NSEL,S,LOC,X,0.75*w,1199        ! Select the nodes at the axis (x=3*w/4)
NSEL,R,LOC,Z,th/2
CM,nodes_major_axis5,NODES      ! Create component

VSEL,S, , ,4,16,4               ! Select volumes 4,8,12 & 16
nslv,s,1                        ! Select all nodes on the volumes
NSEL,R,LOC,X,-1,w+1
NSEL,R,LOC,Z,th/2
CM,nodes_w,NODES                ! Create component
```

```
ASEL,S, , ,33,53,20                    ! Select area 33 & 53
ASEL,A, , ,66                          ! Select area 66
ASEL,A, , ,70                          ! Select area 70
nsla,s,1                               ! Select all nodes on the areas
NSEL,R,LOC,Z,th/2
CM,nodes_bottom_middle_axis,NODES      !Create component

ASEL,S, , ,11,24,13                    ! Select area 11 & 24
ASEL,A, , ,36                          ! Select area 36
ASEL,A, , ,41                          ! Select area 41
nsla,s,1                               ! Select all nodes on the areas
NSEL,R,LOC,Z,th/2
CM,nodes_top_middle_axis,NODES         ! Create component

ASEL,S, , ,33,53,20                    ! Select area 33 & 53
ASEL,A, , ,66                          ! Select area 66
ASEL,A, , ,70                          ! Select area 70
nsla,s,1                               ! Select all nodes on the areas
NSEL,R,LOC,Z,th/2
NSEL,R,LOC,X,w/2
CM,nodes_bottom_central,NODES          ! Create component

ASEL,S, , ,11,24,13                    ! Select area 11 & 24
ASEL,A, , ,36                          ! Select area 36
ASEL,A, , ,41                          ! Select area 41
nsla,s,1                               ! Select all nodes on the areas
NSEL,R,LOC,Z,th/2
NSEL,R,LOC,X,w/2
CM,nodes_top_central,NODES             ! Create component

ASEL,S, , ,47,51,4                     ! Select area 47 & 51
ASEL,A, , ,56                          ! Select area 56
ASEL,A, , ,69                          ! Select area 69
nsla,s,1                               ! Select all nodes on the areas
NSEL,R,LOC,Z,th/2
CM,nodes_contact_bottom_middle_axis,NODES      !Create component

ASEL,S, , ,18,22,4                     ! Select area 18 & 22
ASEL,A, , ,27                          ! Select area 27
ASEL,A, , ,39                          ! Select area 39
nsla,s,1                               ! Select all nodes on the areas
NSEL,R,LOC,Z,th/2
CM,nodes_contact_top_middle_axis,NODES     !Create component

! DEFINE CONSTRAINTS !

cmsel,s,nodes_top                      ! Select component
d,all,uy,-1                            ! Displacement at the top of -1 in Y axis
cmsel,s,nodes_top_central              ! Select component
d,all,ux,0                             ! Displacement at the top of 0 in X axis

cmsel,s,nodes_top_middle_axis          ! Select component
d,all,uz,0                             ! Displacement at the top middle axis of 0 in Z axis
cmsel,s,nodes_bottom                   ! Select component
d,all,uy,0                             ! Displacement at the bottom of 0 in Y axis
cmsel,s,nodes_bottom_central           ! Select component
d,all,ux,0                             ! Displacement at the bottom of 0 in X axis
cmsel,s,nodes_bottom_middle_axis       ! Select component
d,all,uz,0                             ! Displacement at the bottom middle axis of 0 in Z axis
```

```
! CREATE THE CONTACT ELEMENTS !
/COM, CONTACT PAIR CREATION - START
CM,_NODECM,NODE
CM,_ELEMCM,ELEM
CM,_KPCM,KP
CM,_LINECM,LINE
CM,_AREACM,AREA
CM,_VOLUCM,VOLU
/GSAV,cwz,gsav,,temp
MP,MU,1,
MAT,1
MP,EMIS,1,7.88860905221e-031
R,3
REAL,3
ET,3,170
ET,4,174
R,3,,,1.0,0.1,0,
RMORE,,,1.0E20,0.0,1.0,
RMORE,0.0,0,1.0,,1.0,0.5
RMORE,0,1.0,1.0,0.0,,1.0
KEYOPT,4,4,0
KEYOPT,4,5,0
KEYOPT,4,7,0
KEYOPT,4,8,0
KEYOPT,4,9,1
KEYOPT,4,10,2
KEYOPT,4,11,0
KEYOPT,4,12,0
KEYOPT,4,2,0
KEYOPT,3,5,0
NSEL,S,,,NODES_CONTACT_BOTTOM   ! Generate the target surface
CM,_TARGET,NODE
TYPE,3
ESLN,S,0
ESURF
CMSEL,S,_ELEMCM
NSEL,S,,,NODES_CONTACT_TOP      ! Generate the contact surface
CM,_CONTACT,NODE
TYPE,4                          ! Lagrange method
ESLN,S,0
ESURF
ALLSEL
ESEL,ALL
ESEL,S,TYPE,,3
ESEL,A,TYPE,,4
ESEL,R,REAL,,3
/PSYMB,ESYS,1
/PNUM,TYPE,1
/NUM,1
EPLOT
ESEL,ALL
ESEL,S,TYPE,,3
ESEL,A,TYPE,,4
ESEL,R,REAL,,3
CMSEL,A,_NODECM
CMDEL,_NODECM
CMSEL,A,_ELEMCM
CMDEL,_ELEMCM
CMSEL,S,_KPCM
CMDEL,_KPCM
```

```
CMSEL,S,_LINECM
CMDEL,_LINECM
CMSEL,S,_AREACM
CMDEL,_AREACM
CMSEL,S,_VOLUCM
CMDEL,_VOLUCM
/GRES,cwz,gsav
CMDEL,_TARGET
CMDEL,_CONTACT
/COM, CONTACT PAIR CREATION - END
/COM, CONTACT PAIR PROPERTIES - START
KEYOPT,4,2,4
/COM, CONTACT PAIR PROPERTIES - END
ALLSEL,ALL
```

APPENDIX B. MATLAB code

B.1. Contact pressure distribution

The MATLAB code used for defining the pressure distribution, from both the analytical and numerical results, is presented here.

```
clear all
close all

% Import reaction force at the bottom (Fy)
P_0 = importfile2('Fy_bottom.txt', 2430, 2430);

%% Analytical results

w = 1550E-6;                    % Flat punch (m)
R = 3*w;                        % Radius (m)
a = w/2;                        % Half of flat punch (m)
E= 2.05E11;                     % Young's Modulus (Pa)
nu = 0.3;                       % Poisson ratio
th = 5*w;                       % Thickness (m)
P = P_0/th;                     % Load per unit length

E_ast = 1/((2/E)*(1-nu^2));     % eq. 3.3
eq_1_part1 = (2*P*R)/(a^2*E_ast);   % eq. 3.1 part 1

% Graphical solution for fi_0
x = [0:2*pi/10000:2*pi];
for t = 1:length(x)
   if (x(t)==pi)|(x(t)==2*pi)   % 'if' loop to avoid infinite
      x(t) = 1.001*x(t);
   end
curve(t) = (pi-2*x(t))/(2*(sin(x(t)))^2) - cot(x(t));
diff(t) = curve(t)-eq_1_part1;
end

[minimum,idx] = min(abs(diff));
fi_0 = x(idx);

b = a/sin(fi_0);
x = [0:b/10000:b];

for i = 1:length(x)
   if x(i) == w/2               % 'if' loop to avoid NaN
      x(i) = 1.001*x(i);
   end
   fi = asin(x(i)/b);
   eq_17_part1 = (2/pi)/(pi-2*fi_0-sin(2*fi_0));
   eq_17_part2 = (pi-2*fi_0)*cos(fi)+log((abs(sin(fi+fi_0)/sin(fi-
fi_0)))^sin(fi)*(abs(tan((fi+fi_0)/2)*tan((fi-fi_0)/2)))^sin(fi_0));
   pressure(i)=(P/b)*(eq_17_part1)*eq_17_part2;
end

x_um1 = 10^6*x + 775;
x_um2 = -10^6*x + 775;

% Plot analytical results
figure()
plot(x_um1,pressure/10^6,'blue')
```

```
hold on
plot(x_um2,pressure/10^6,'blue')
title('Contact pressure CASE 1 (Analytical) Uy=-25{\mu}m')
xlabel('X position [{\mu}m]')
ylabel('Contact Pressure [MPa]')

%% Numerical results
w = 1550;                          % Flat punch (µm)
th = 5*w;                          % Thickness (µm)

% Import node contact position (1 Node ID, 2 pos X, 3 pos Y, 4 pos Z)
node_pos_contact = importfile1('mid_line_contac_nodes.txt', 4, 164);
% Import contact pressure (1 Node ID, 2 STAT, 3 PENE, 4 PRES, 5 SFRI)
ContactPressure = importfile4('nodal_contact_pressure.txt', 9, 1552);

% Add position at the end of ContactPressure
i = 1;
for i = 1:length(ContactPressure(:,1))
   c = 1;
   nodeID = ContactPressure(i,1);
   while c <= length(node_pos_contact(:,1))
      if node_pos_contact(c,1) == nodeID
         ContactPressure(i,6) = node_pos_contact(c,2);
         ContactPressure(i,7) = node_pos_contact(c,3);
         ContactPressure(i,8) = node_pos_contact(c,4);
         c=c+1;
      else
         c=c+1;
      end
   end
end

% Sort de matrix by pos X
[C11,e1] = sort(ContactPressure(:,6));
C11 = [ContactPressure(e1,1) ContactPressure(e1,2) ContactPressure(e1,3)
ContactPressure(e1,4) ContactPressure(e1,5) C11 ContactPressure(e1,7)
ContactPressure(e1,8)];

% Take only the nodes in the middle plane
C1 = [];
for i = 1:length(C11(:,8))
   if round(C11(i,8),1) == round(th/2,1)
      C1(end+1,:) = C11(i,:);
   end
end

% Plot numerical results
figure()
plot(C1(:,6),C1(:,4)*1000000)
title('Contact pressure CASE 1 (Numerical) Uy = -25um')
xlabel('X position [{\mu}m]')
ylabel('Contact Pressure [MPa]')

% Comparison analytical and numerical results
figure()
plot(x_um1,pressure/10^6,'blue')
hold on
plot(x_um2,pressure/10^6,'blue')
hold on
plot(C1(:,6),C1(:,4)*10^6,'red')
```

```
title('Analytical & Numerical Results Uy = -25um for 60 elements')
xlabel('X position [{\mu}m]')
ylabel('Contact Pressure [MPa]')
legend('Analytical case 1','Analytical case 1','Numerical case 1')
```

B.2. Contact stiffness using relative displacement

The MATLAB code used for plotting the numerical results of contact stiffness distribution for one axis using relative displacement is presented here. In this example, the normal contact stiffness is found.

```
clear all
close all

w = 1550;                    % Flat punch (μm)
th = 5*w;                    % Thickness (μm)

% Import reaction force at the bottom surface
Fy = importfile2('Fy_bottom.txt', 1378, 1378);
Fy = Fy/th;                                          % Load per unit length

% Import nodes displacements
Read_nodes = importfile('Uy_disp.txt', 11, 159);
% Import nodes position
Nodepos = importfile1('node_pos.txt', 4, 131);
nodeposY = [nodepos(:,1) nodepos(:,3)];

% Sort matrix by pos Y (1 node ID, 2 pos Y, 3 Uy)
[B,k] = sort(nodeposY(:,2));
B = [Read_nodes(k,1) B Read_nodes(k,2)];

Uy = B(:,3); % Displacements vector

k = []; % K
pos_nodesy = []; % Nodes position
for i = 2:length(Uy)
   dis = Uy(i)-Uy(i-1);
   if dis==0
      k1 = k(i-1);
      pos_nodesy(i)= pos_nodesy(i-1);
   else
      k1= abs(Fy/dis);
      pos_nodesy(i)=(B(i,2)+B(i-1,2))/2;
   end
   k(i)= k1;
end
k(1)=[];
pos_nodesy(1)=[];

% Plot results
figure()
plot(k,pos_nodesy)
title('Normal contact stiffness for the Y axis')
xlabel('Contact stiffness [N/μm/μm]')
ylabel('Y position [μm]')
```

B.3. Contact stiffness using strain

The MATLAB code used for plotting the numerical results of contact stiffness distribution for one axis using elastic strain is defined here. The following example shows the normal contact stiffness.

```
clear all
close all

w = 1550;
th = 5*w;

% Import reaction force at the bottom surface
Fy = importfile2('Fy_bottom.txt', 1378, 1378);
Fy = Fy/th;                                          % Load per unit length


% Import nodes deformation (1 node ID, 2 Strain x, 3 Strain y)
Read_nodes = importfile5('Ey.txt', 13, 6561);
% Import nodes position (1 Node ID, 2 Pos X, 3 Pos Y, 4 Pos Z)
nodepos = importfile1('node_pos.txt', 4, 131);

% Sort matrix by Node ID
[Ey_ordered,k1o] = sort(Read_nodes(:,1));
Ey_ordered = [Ey_ordered Read_nodes(k1o,2) Read_nodes(k1o,3)];

% Matrix with all heights and the average value of Ex and Ey for each node (1 Node ID, 2
Ex, 3 Ey)
Average = [];
i = 1;                      % Go through Ey_ordered (find all possible pos Y)
d = 1;                      % All possible heights (rows of Average)
c = 1;                      % Go throught Ey_ordered (Add Uy and make the average)
while i<=length(Ey_ordered(:,1))
   NodeID = Ey_ordered(i,1);
   Average(d,1) = NodeID;
   Average(d,2) = 0; %Ex
   Average(d,3) = 0; %Ey
   a = 1;                   % Ends while and counts nodes with that pos Y
   while c<=(length(Ey_ordered(:,1))+1) && a>=0
      if c==(length(Ey_ordered(:,1))+1)
         Average(d,2) = Average(d,2)/(a-1);
         Average(d,3) = Average(d,3)/(a-1);
         a = -1;
      elseif Ey_ordered(c,1) == NodeID
         Average(d,2) = Average(d,2)+Ey_ordered(c,2);
         Average(d,3) = Average(d,3)+Ey_ordered(c,3);
         a = a+1;
         c = c+1;
      else
         Average(d,2) = Average(d,2)/(a-1);
         Average(d,3) = Average(d,3)/(a-1);
         a = -1;
      end
   end
   i = c;
   d = d+1;
end

% Add Ex and Ey: 1 Node ID, 2 Pos X, 3 Pos Y, 4 Pos Z, 5 Ex, 6 Ey
```

```
for i=1:length(Average(:,1))
   for c=1:length(nodepos(:,1))
   if Average(i,1)==nodepos(c,1)
      nodepos(c,5) = Average(i,2);
      nodepos(c,6) = Average(i,3);
      c = length(nodepos(:,1))+10;
   end
   end
end

% Sort de matrix by pos Y
[B,k] = sort(nodepos(:,3));
B = [nodepos(k,1) nodepos(k,2) B nodepos(k,4) nodepos(k,5) nodepos(k,6)];

pos_nodesy = B(:,3);          % Nodes position Y
Ex = B(:,5);                  % Strain X
Ey = B(:,6);                  % Strain Y

k = [];                       % K
for i=1:length(Ey)
   k(i) = abs(Fy/Ey(i));
end

% Plot results
figure()
plot(k1,pos_nodesy1)
title('Normal contact stiffness for the Y using strain')
xlabel('Contact stiffness [N/µm/µm]')
ylabel('Y position [µm] ')
```

B.4. Shear stress distribution

The MATLAB code used for defining the shear stress distribution, from both the analytical and numerical results is presented here.

```
clear all
close all

% Reaction forces at the bottom (Fy and Fx)
P_0 = importfile2('Fy_bottom_C3new.txt', 2574, 2574);
Q_0 = importfile3('Fx_bottom_C3new.txt', 2574, 2574);

% Parameters for the analytical results
w = 1550E-6;                  % Flat punch (m)
R = 3*w;                      % Radius (m)
a = w/2;                      % Half of flat punch (m)
E= 2.05E11;                   % Young's Modulus (Pa)
nu = 0.3;                     % Poisson ratio
mu = 0.5;                     % Friction coefficient
P = P_0/(5*w);                % Normal load per unit length
Q = abs(Q_0/(5*w));           % Tangential load per unit length

E_ast = 1/((2/E)*(1-nu^2));   % eq. 3.3

%% Pressure distribution p(x)
eq_1_part1 = (2*P*R)/(a^2*E_ast); % eq. 1 part 1

% graphical solution for fi_0
```

```
x=[0:2*pi/1000:2*pi];
for t=1:length(x)
   if (x(t)==pi)|(x(t)==2*pi)      % 'if' loop to avoid infinite
      x(t)=1.001*x(t);
   end
curve(t)=(pi-2*x(t))/(2*(sin(x(t)))^2) - cot(x(t));
diff(t)=curve(t)-eq_1_part1;
end

[minimum,idx] = min(abs(diff));
fi_0 = x(idx);
b = a/sin(fi_0);

%% Shear stress distribution (q*(x))
eq_1_part1_1 = ((2*P*R)/(a^2*E_ast));      % eq. 5.4 part 1.1
eq_1_part1_2 = 1-Q/(mu*P);                 % eq. 5.4 part 1.2
eq_1_part1 = eq_1_part1_1*eq_1_part1_2;    % eq. 5.4 part 1

% graphical solution for theta_0
x=[0:2*pi/10000:2*pi];
for t=1:length(x)
   if (x(t)==pi)|(x(t)==2*pi)      % 'if' loop to avoid infinite
      x(t)=1.001*x(t);
   end
curve(t)=(pi-2*x(t))/(2*(sin(x(t)))^2) - cot(x(t));
diff(t)=curve(t)-eq_1_part1;
end

[minimum,idx] = min(abs(diff));
theta_0 = x(idx);
c = a/sin(theta_0);

x=[0:c/1000:c c+c/1000:c/1000:b];
for i=1:length(x)
   if x(i) == w/2                  % if loop to avoid NaN
      x(i) = 1.001*x(i);
   end
   fi= asin(x(i)/b);
   eq_17_part1 = (2/pi)/(pi-2*fi_0-sin(2*fi_0));
   eq_17_part2 = (pi-2*fi_0)*cos(fi)+log((abs(sin(fi+fi_0)/sin(fi-
fi_0)))^sin(fi)*(abs(tan((fi+fi_0)/2)*tan((fi-fi_0)/2)))^sin(fi_0));
   pressure(i)=(P/b)*(eq_17_part1)*eq_17_part2;
end

for i=1:length(x)
   if x(i) == w/2                  % if loop to avoid NaN
      x(i) = 1.001*x(i);
   end
   theta= real(asin(x(i)/c));
   eq_17_part1 = (2/pi)/(pi-2*theta_0-sin(2*theta_0));
   eq_17_part2 = (pi-2*theta_0)*cos(theta)+log((abs(sin(theta+theta_0)/sin(theta-
theta_0)))^sin(theta)*(abs(tan((theta+theta_0)/2)*tan((theta-theta_0)/2)))^sin(theta_0));
   shear(i)=((mu*P-Q)/c)*eq_17_part1*eq_17_part2;
end

%% Stress distribution q(x) = mu*p(x)-q*(x)
final = mu*pressure-shear;

x_um1 = 10^6*x + 775;
x_um2 = -10^6*x + 775;
```

```
%% Plot analytical results
figure()
plot(x_um1,(final/10^6),'blue')
hold on
plot(x_um2,(final/10^6),'blue')
title('Shear stress distribution (Analytical result)')
xlabel('X position [{\mu}m]')
ylabel('Contact shear [MPa]')

%% Numerical results
w = 1550;                % Flat punch (μm)
th = 5*w;                % Thickness (μm)

% The vector C1 is obtained from Appendix B1 (the same procedure is applied to find C3
in this script)

% Import node contact position (1 Node ID, 2 pos X, 3 pos Y, 4 pos Z)
node_pos_contact = importfile1('mid_line_contact_nodes.txt', 4, 3046);
% Import contact pressure (1 Node ID, 2 STAT, 3 PENE, 4 PRES, 5 SFRI)
ContactPressure = importfile5('nodal_contact_pressure.txt', 9, 1703);

% Add position at the end of ContactPressure
I = 1;
for i=1:length(ContactPressure(:,1))
   c = 1;
   nodeID = ContactPressure(i,1);
   while c<=length(node_pos_contact(:,1))
      if node_pos_contact(c,1) == nodeID
         ContactPressure (i,6) = node_pos_contact (c,2);
         ContactPressure(i,7)= node_pos_contact(c,3);
         ContactPressure(i,8)= node_pos_contact(c,4);
         C = c+1;
      else
         c = c+1;
      end
   end
end

% Sort de matrix by pos X
[C33,e3] = sort(ContactPressureCASE3(:,6)); % sort de matrix by Xpos
C33 = [ContactPressureCASE3(e3,1) ContactPressureCASE3(e3,2)
ContactPressureCASE3(e3,3) ContactPressureCASE3(e3,4) ContactPressureCASE3(e3,5)
C33 ContactPressureCASE3(e3,7) ContactPressureCASE3(e3,8)];

% Take only the nodes in the middle plane
C3 = [];
for i=1:length(C33(:,8)) % take ony the nodes in z=th/2
   if round(C33(i,8),1) == round(th/2,1)
      C3(end+1,:)=C33(i,:);
   end
end

%% Comparison of the results
figure()
plot(C3(:,6),C3(:,5)*10^6,'green')
hold on
plot(C1(:,6),C1(:,5)*10^6,'red')
hold on
plot(x_um1,(final)/10^6,'blue')
```

```
hold on
plot(x_um2,(final)/10^6,'blue')
hold on
title('Shear stress distribution for mesh 3 (Numerical results)')
xlabel('X position [{\mu}m]')
ylabel('Shear stress [MPa]')
legend('Numerical case with friction + Uy + Ux','Numerical case with Uy','Analytical case')
```